KAUNAS UNIVERSITY OF TECHNOLOGY

MECHANICAL ENGINEERING AND DESIGN FACULTY

Jacob Shiby Mathew

ANALYSIS OF PROPERTIES OF FUNCTIONAL POLYMERS

Master's Degree Final Project

Supervisor

Assoc. prof. dr. Kazimieras Juzėnas

KAUNAS, 2016

KAUNAS UNIVERSITY OF TECHNOLOGY

MECHANICAL ENGINEERING AND DESIGN FACULTY

Approved:

Head of Mechanical Engineering Department

(Signature, date)

Vytautas Grigas

(Name, Surname)

ANALYSIS OF PROPERTIES OF FUNCTIONAL POLYMERS

Master's Degree Final Project

Title of study programme (code 621H30001)

Supervisor

(signature) Assoc. prof. dr. Kazimieras Juzėnas

(date)

Reviewer

(signature) Assoc. prof. dr. Kristina Žukienė

(date)

Project made by

(signature) Jacob Shiby Mathew

(date)

KAUNAS, 2016

KAUNAS UNIVERSITY OF TECHNOLOGY

Mechanical Engineering and Design
(Faculty)

Jacob Shiby Mathew
(Student's name, surname)

Master's in Mechanical Engineering, 621H30001
(Title of study programme, code)

"Analysis of Properties of Functional Polymers"

DECLARATION OF ACADEMIC INTEGRITY

09 06 2016
Kaunas

I confirm that the final project of mine, **Jacob Shiby Mathew**, on the subject "Analysis of Properties of Functional Polymers" is written completely by myself; all the provided data and research results are correct and have been obtained honestly. None of the parts of this thesis have been plagiarized from any printed, Internet-based or otherwise recorded sources; all direct and indirect quotations from external resources are indicated in the list of references. No monetary funds (unless required by law) have been paid to anyone for any contribution to this thesis.

I fully and completely understand that any discovery of any facts of dishonesty inevitably results in me incurring a penalty under procedure effective at Kaunas University of Technology.

(name and surname filled in by hand) *(signature)*

KAUNAS UNIVERSITY OF TECHNOLOGY
FACULTY OF MECHANICAL ENGINEERING AND DESIGN

Approved:

Head of Mechanical Engineering Department _____ *(Signature, date)*
Vytautas Grigas
(Name, Surname)

Head of Study Programmes in the Field of Mechanical Engineering _____ *(Signature, date)*
Kęstutis Pilkauskas
(Name, Surname)

MASTER STUDIES FINAL PROJECT TASK ASSIGNMENT
Study programme MECHANICAL ENGINERING - 621H30001

Approved by the Dean's Order No.V25-11-7 of May 3rd , 2016 y

Assigned to the student Jacob Shiby Mathew
(Name, Surname)

1. Title of the Project

Analysis of Properties of Functional Polymers

2. Aim of the project

To study and analyze the properties of functional polymers, its testing & applications.

3. Tasks of the project

1. Analysis of Tribo-testing methods and possibilities of functional polymer applications.
2. Analysis of Tribo-testing equipment for testing functional polymers.
3. Experimental testing of tribological properties in functional polymer-UHMWPE.

4. Specific Requirements

None

5. This task assignment is an integral part of the final project

6. Project submission deadline: 2016 May 20th.

Task Assignment received Jacob Shiby Mathew
(*Name, Surname of the Student)* (*Signature, date*)

Supervisor Assoc. prof. dr. Kazimieras Juzėnas
(*Position, Name, Surname*) (*Signature, date*)

ACKNOWLEDGEMENT

Principally I would like to thank *GOD the Triune*, for the grace that was bestowed upon me, only because of which this quest has been accomplished.

I would like to thank *Kaunas University of Technology (KTU)*, for all the facilities and services provided to me during the course of my Master Study. I am thankful to the *Faculty of Mechanical Engineering and Design* for giving me this opportunity. I am deeply grateful to my supervisor *Assoc. Prof. Dr. Kazimieras Juzėnas* for guiding me over the course of my study program without whom this would not have been possible. I am also thankful to *Assoc. Prof. Dr. Kristina Žukienė* for reviewing my Thesis report.

I acknowledge the *University of Ljubljana (UL)*, at which I was an Erasmus+ exchange student, wherein I had garnered priceless experiences. My special thanks to *Prof. Dr. Mitjan Kalin* for having me at the *Laboratory for Tribology and Interface Nanotechnology (TINT)*, as for my Erasmus+ traineeship which had been a central and an essential factor in the construction of my Master Thesis. I am enormously indebted to *Dr. Alja Kupec* for patiently listening to my perspectives, meticulously guiding me and selflessly teaching me research, during the course of my stay at *TINT*. I would also like to thank the other researchers at *TINT* for their contribution.

I express my deep gratitude towards my wonderful *parents* and my dear *sister* for their prayers, encouragement and support, and who have also been the supporting pillars of my life. I am obliged to thank all my admirable *friends* from around the globe for motivating me and for their sincere wishes & prayers in this pursuit of mine.

Thank you Everybody!!

Dedicating this to You All!!

TABLE OF CONTENTS

LIST OF FIGURES

LIST OF TABLES

LIST OF ABBREVIATIONS

Abbreviation	*Meaning*
ABS	Acronitrile-Butadiene Styrene
ALN	Alendronate Sodium
ASTM	American Society for Testing and Materials
AVG.	Average
COF	Coefficient of Friction/ Friction Coefficient
DSC	Differential Scanning Calorimetry
EP	Epoxy Resin
GO	Graphene Oxide
HDPE	High-Density Polyethylene
LDPE	Low-Density Polyethylene
MWCNT	Multi-Wall Carbon Nano Tube
NWR	Normalized Wear Rate
PA	Polyamide
PBT	Polybutylene Terephthalate
PE	Polyethylene
PEEK	Polyether-ether-ketone
POM	Polyoxymethylene
PTFE	Polytetrafluoroethylene
SAE	Society of Automotive Engineers
SBR	Styrene-Butadiene Rubber
STD. DEV.	Standard Deviation
TGA	Thermogravimetric Analysis
TTS	Tribological Transformed Structure
UHMWPE	Ultra-High Molecular Weight Polyethylene
UPD	Unidirectional-Perpendicular
UPL	Unidirectional-Parallel

Jacob Shiby Mathew. Funkcinių polimerų savybių tyrimas. *Magistro baigiamasi projektas* /vadovas doc. dr. Kazimieras Juzėnas; Mechanikos inžinerijos ir dizaino fakultetas , Kauno technologijos universitetas.

Studijų kryptis ir sritis: technologijos mokslai, mechanikos inžinerija

Reikšminiai žodžiai: *funkciniai polimerai, tribologinės savybės, tribologinė įranga*.

Kaunas, 2016. 63 p.

SANTRAUKA

Funkcinių polimerų reikšmė šiuolaikinėje visuomenėje. Tai daugiausiai įtakojama gerų polimerų savybių: plataus lydymosi temperatūrų diapazono, nedidelio susitraukomo stingstant, palyginus gero atsparumo karščiui ir smūgiams, atsparumo cheminiam poveikiui ir matmenų stabilumo. Apart šių savybių, mažas trinties koeficientas, atsparumas dilimui, atsparumas smūgiams, tamprumas, nedidelė santykinė masė ir kaina, lyginat su kitomis medžiagomis (ypač metalais), leidžia polimerus naudoti skirtingose srityse.

Šiame darbe yra nagrinėjamos funkcinių polimerų tribologinėse savybės (trinties ir dilimo), siekiant išanalizuoti jų praktinio panaudojimo galimybes. Yra išanalizuoti tribologinių tyrimų metodai ir įranga, jos panaudojimo privalumai ir apribojimai. Praktiniams taikymams yra siekiama pagaminti polimerus, pasižyminčius mažu trinties koeficientu ir atsparumu dilimui. Matuojant trinties koeficientą ir santykinį dilimo intensyvumą buvo tiriama polimerų apdorojimo procesų įtaka jų tribologinėms savybėms. Tyrimų rezultatai parodė, kad papildomas vakuuminis polimerų apdorojimas leidžia gauti geresne tribologines bandinių paviršių savybes. Tuo metu prailgintas polimerizacijos laikas pablogino šias savybes. Elementai pagaminti panaudojus kietinimą vakuume gali būti naudojami polimerinių guolių, kurie bus naudojami sunkiomis eksploatacijos sąlygomis, gamybai.

Jacob Shiby Mathew. Analysis of Properties of Functional Polymers. *Master's in Mechanical Engineering* Final Project / supervisor assoc. prof. dr. Kazimieras Juzėnas; Faculty of Mechanical Engineering and Design, Kaunas University of Technology.

Study area and field: Technological Sciences, Mechanical Engineering,

Keywords: *Functional Polymers, Tribological Properties, Tribo-Machinery.*

Kaunas, 2016. 63 p.

SUMMARY

Functional polymers are of immense significance to the society. This is fundamentally because of its natural properties such as a broad range of melting points, reduced mold-shrinkage, fairly good heat and impact resistance, good chemical resistance and dimensional stability of which one or more specific properties would be a highlighting factor for its use in applications. In addition to this other factors such as low friction, wear resistance, shock-loading accommodation, elasticity, low weight and cost in comparison to other materials (metals) makes it quite ideal to use in different areas. Here in this study, tribological properties such as friction and wear have been analyzed in functional polymers with an idea to extend the knowledge to real-life application. Tribo-machinery and its functioning is studied and described in detail. Different types of Tribo-machines are analyzed and thus merits & demerits are perceived. Analysis of the effect of final-processing conditions of a functional polymer (UHMWPE) is done and tribological properties such as coefficient of friction (COF) and normalized wear rate (NWR) are done. It has been observed that it is quite ideal to have in applications, a functional polymer with low friction coefficient and low degree of normalized wear rate. Polymer post-processing by vacuum cooling was observed to produce superior surface and tribological properties but post-processing by prolonged cooling worsened the material properties in general. The vacuum cooled functional polymer is proposed to be put to practice in high-performance bearings.

INTRODUCTION

Functional polymers are long chain molecules with a definite property that makes it stand out for its employment in different applications. They are also one among the imperatively researched areas in the field of material science, currently. This is fundamentally because of the extensive amount of variations in material properties that can be done which makes it multi-functional. Basically they form a basis in most lifecycle processes. For instance they are a part of our food, shelter and the human body.

To synthesize functional polymers and its variants, it is important to study its properties and dependency on external conditions. The use of functional polymers which is quite an increasing trend in tribological applications is attributed to its properties such as low friction and wear resistance. However, tribology when considered in polymers is quite different when compared to metals. Polymers by nature are viscoelastic and possess time dependent properties. What is quite intricate about polymer study is its influence and behavioral change experienced with different operating and environmental conditions. The meritorious aspect of the polymeric interface is that its properties can be metamorphosed by the action of both physical and chemical techniques to make it appropriate for a particular condition. A functional polymer is typically expected to stay wear resistant with nominal values of friction coefficient with time, this may not always be the case. Thus improvements can be done by virtue of lubrication and/or by adding filler materials that are well researched in that specific regard. Therefore properties like friction and wear-resistance can be fine-tuned.

With functional polymers there are the merits of easier processing, decreased costs, a wide span of material properties and research perspectives. This has resulted in multiple tribological systems containing functional polymers. In recent years there have been studies on plastic tribology, polymer-composite tribology and rubber tribology. In the view of the extensive applications of functional polymers, an understanding on the polymer tribology is quite indispensable. [1-4]

AIM AND TASK FORMULATION

Most areas of applications nowadays require advanced research due to essentialities of customized demands and property-improvement exigencies. One method is to employ functional polymers and thereby the necessity to materialize properties of functional polymers to adapt to these conditions is quite important. The tribological properties of polymers like friction and wear also depend upon how it is processed.

The aim would be to analyze the tribological properties of functional polymers so as to propose it in possible applications. Presented below are the **tasks that are undertaken.**

1 Analysis of Tribo-testing methods and possibilities of functional polymer applications.
2 Analysis of Tribo-testing equipment for testing functional polymers.
3 Experimental testing of tribological properties in functional polymer-UHMWPE.

1 CHARACTERISTICS OF FUNCTIONAL POLYMERS

1.1 TYPICAL PROPERTIES OF FUNCTIONAL POLYMERS

Functional polymers are materials with a very distinct and specific property which makes its utilization for different applications. There are significant differences in the wear mechanisms and the friction coefficients between metallic and polymeric materials. The differences can be put to use in producing subjects such as new bearings materials which can attribute to improved tribological performance. A common polymeric material such as PTFE, has a friction coefficients as low as 0.05 in the absence of any kind of lubricant which is quite an advantage. In general, the development of new technologies is stimulated by factors such as environmental pollution, need for wear resistant materials, weight considerations, energy usage etc. Polymers are associated with hydrocarbon-polymerization and there are a number of substances that can be produced by working on its chemical properties. A few of the most common polymers used in tribological applications and its specific properties are depicted in table 1.1. [1-4]

Table 1.1. Specific Properties of Functional Polymers [2]

Polymer	Specific Properties
PTFE	Low Friction, High Wear Rate, High Operating Temperature Limits
PEEK	Resistance to Chemical Reagents, High Operating Temperature and COF
UHMWPE	Very High Wear Resistance, Good Abrasive Resistance, Moderate COF
Polyurethane	Good Resistance to Abrasive Wear, Relatively High COF in Sliding
Polyimides	High Contact Stresses, High Operating Temperatures, High Performance Polymer
Nylons	Moderate COF, Low Wear Rate, Medium Performance Bearing Material
Polyacetals	Similar Performance to Nylon, Durability in Rolling Contacts

Most of these materials were never initially intended to be used as in bearing or wear resistant materials but due to its tribological properties as described in the table 1.1, makes it a good option.

Typically high operating temperatures in polymers typically refer to temperatures in the range that exceeds 150°C. Most polymers used in engineering applications are blends, for instance; nylon containing PTFE which is beneficial in friction control. The thermal and mechanical properties of some of the functional polymers are depicted in table 1.2. [2-6]

Table 1.2. Thermal and Mechanical Properties of Functional Polymers [2]

Polymer	**Upper Service Temperature, [°C]**	**Thermal Conductivity, [W/mK]**	**Thermal Expansivity, [x10^{-6} K^{-1}]**	**Tensile Modulus, [GPa]**	**Tensile Strength, [MPa]**
PTFE	260	0.25	130	0.5	10
PEEK	250	0.25	60	2.2	85
UHMWPE	95	0.45	170	0.2-1.2	20
Polyimides	250-320	0.2	50	2.5	70
Nylons	110-180	0.25	90	3.3	82
PC	125	0.2	70	2.4	65

1.2 BASIC ANALYSIS OF FUNCTIONAL POLYMERS

Talking about functional polymers, a polymer PEEK (Polyether-ether-ketone) capable of withstanding high temperatures and excellent mechanical properties is used in applications such as bearings, fuel filters, pistons etc. But there is always the need for improvement in functionality of the polymer. For instance, PTFE (Polytetrafluoroethylene) when infiltrated into PEEK produces improved frictional properties in the native polymer PEEK. The effect of friction is most likely dependent on the molecular-kinetic processes in the contact zone of reference. Another polymer, UHMWPE (Ultra-high-molecular weight polyethylene) has very high wear resistance and fine abrasive resistance. In most cases the applications have sliding contacts against metals or alloys. Steel is one among them and sliding of UHMWPE against steel produces a polymeric surface layer. The general effect of sliding speed on the friction and wear properties is contributed to interfacial temperatures. Additionally, with increase in surface roughness at a higher sliding speed, raises the friction coefficient and temperature of the interface. [7-10]

It had been observed by S.W. Zhang [10] that the leanest superficial layer of UHMWPE when sliding against steel was up to a range corresponding to 2 nm. And this superficial layer in the tribological transfer of material during sliding contact contained oxidized fragments of the polymer and iron which typically formed cluster-like structures. This predominantly played an imperative role in the tribo-chemical process. Roughness is another measure of how distinctively surface parameters play a role in polymer-tribology. Considering polyacetals such as PE (Polyethylene), PA (Polyamide), PC (Polycarbonate) and EP (Epoxy resin), it was observed that the COF in these polyacetals when slid against an S45C steel, decreased with increase in surface roughness. To a predominant extent the COF of polymers depend on the factor relating to interfacial adhesion. [2]

In polymer-tribology there is always transfer of material from the soft body to the hard. This involves shearing of the interlamellar structures and results in the formation of a transfer film. When this happens, the orientation of the distorted structure, crystallite size and degree of crystallinity of the polymer after the process sliding is significantly contrast when compared to the native condition. [10-14]

To improve the friction and wear properties, sometimes lubrication is employed. PEEK was not found to behave feasibly as in lubrication of sliding contacts, instead the effects were detrimental. Atmospheric humidity influences the polymer-tribology in sliding contact pair of a polymer-metal type. HDPE (High-density polyethylene) and PTFE (Polytetrafluoroethylene) were some of the polymers with wear effects due to atmospheric humidity. In the context of the wear process, there is also transfer film formation (superficial polymeric layer) but the film degrades by thermos-activation mechanism. [15-17]

Low values of activation energy is related to disassociation of intermolecular bonds that are weak, coupled with interplanar slipping and shearing action in the polymeric lump. To study the thermal behavior of wear processes that relates to formation of debris , tests such as DSC (Differential Scanning Calorimetry) and TGA (Thermogravimetric Analysis) are employed. The average frictional temperatures in the sliding interface span from 300 – 345 °C. Wear behavior is typically related to factors such as plastic flow, fatigue-delamination, microcutting etc. [10] [18-21]

1.3 APPLICATIONS OF FUNCTIONAL POLYMERS

The properties of functional polymers such as self-lubricating behavior, chemical inertness and low wear rate at dry friction have been instrumental in their use in tribological applications.

Polymers such as PTFE under heavy loads and low velocities of sliding have still a low friction coefficient which is quite a merit. Thus this make PTFE eligible for applications such as sliding bearing also considering its self-lubricating properties. Anti-friction PTFE-based materials (soot, coke, metal fibers, molybdenum disulphide etc.) improve the properties of the polymer-matrix in many cases. Polyamides (PA) are used in fabrication of sliding bearings with reinforcing fillers and dry lubricants. They also find good application in polymer gears and thin polymer coatings. Polyolefins are typically put to practice in matrices relating to anti-friction composites. Polymers such as polyformaldehyde, polycarbonate and polyarylate also find applications in polymer gears, sliding bearings and bushings. Polyimidies have an important role in applications relating to higher operating temperatures such as 220 -260 °C. Certain anti-friction applications also contain epoxy and phenol-resins as matrices. With the addition of lubricants like molybdenum-disulphide and graphite, its applications can be found in linings of machine guides, brake-materials, clutches etc. Polymers such as polyurethane and rubbers are used as anti-abrasion linings of metal surfaces, contact seals and automotive tires. [22]

Polymers such as UHMWPE can be used in bearing materials, in off-shore applications that are typically characterized by large contact areas, low velocities of sliding and high degree of normal loading. [23] Generally, materials are chosen on cost factors or basic-performance grounds such as nominal flexural modulus, heat deflection temperature etc. Traditionally, there was a fair physical difference in the power transmission and motion transmission modules. But nowadays this distinction is becoming lesser with polymeric applications as integrating elements of drive trains being designed with larger power transmission systems. Thus applications of this sort require low cost, low maintenance, preferably non-lubricated conditions, and simple in design. For these reasons the choice of polymers are a good option. They can be produced easily at a low cost and high production-rates. [24]

Polymers can bring to merits to applications such as gears; less noise, restrained inertia, production flexibility and unacquainted lubricant usage [25]. Another advantage of polymer gears is that it typically requires no finishing process. The savings can be from 10 -50 %, due to low weight and inertia which reduces dynamic loading and noise. Another advantage is that that one-piece parts with internal features could be made, which would rather be difficult in metals. In some applications the chemical resistance of the polymeric material can be superlative to metallic gears in terms of corrosion problems. [26] In the past decade, the use of internally-lubricated thermoplastics in gears has proliferated. Thermoplastic gears are capable of withstanding challenging environmental conditions such as high temperatures, elevated loads etc. Another advantage is that it can quite easily

be reproduced and manufactured using injection molding thereby providing economic advantage in comparison to metallic counterparts, however there are limitations such as fatigue and lack of very-high temperature resistance. [27]

When delving deeper into the process-capabilities of the polymeric gears over the metallic gears, it is observed to have improved dry running capabilities, cost & weight efficiency and smooth running characteristics. When thermoplastics in gears are considered, polymers such as PA, POM, PBT, PE are the commonly used materials. POM for instance provides excellent dimensional accuracy combined with good wear characteristics. But in comparison to metallic counterparts the highlighting demerits would be lower mechanical load resistance, high thermal expansion coefficient and lower operation temperature. One of the most common failure mechanisms in polymer gears would be tooth thickness contraction due to wear, thermal overloading that might cause melting and breakage of tooth-root due to excessive mechanical load. These generally appear in cases of high-load transmission in the absence of external lubrication or any kind of cooling. [28]

2 ANALYSIS OF FRICTION AND WEAR OF FUNCTIONAL POLYMERS

2.1 FRICTION CHARACTERISTICS OF FUNCTIONAL POLYMERS

Friction characteristics in functional polymers can be changed or varied depending on the effects of sliding pair and operating parameters. The force associated with friction is quite closely related to the process-happenings in the thin-surface layer of bodies that interact. The fundamental difference in metals and polymers is the property of a polymeric material to exhibit both elastic and viscous properties upon deformation or stress. Adhesion is an imperative feature of these processes. The sum of the junctional contacts make up the net real area of contact. During the sliding processes the origination of interfacial junctions are typically impacted by the following parameters: [29]

- Contact Area Nature
- Surface Chemistry
- Surface Layer Stress
- Loading Conditions

Strength properties of most thermoplastics appear to change with temperature and quite evidently somewhere close to the glass transition temperature (temperature at which the polymer metamorphoses from a hard, glassy material to a soft, rubbery material). In addition to adhesion there is also deformation that is caused by the presence of asperities on the counterface (hard material against which the polymer slides) making way into the polymer in the polymeric-counterface medium. Therefore there is a definite dissipation of mechanical energy depending upon factors such as sliding conditions, mechanical properties of the polymer, external or environmental conditions etc. Ploughing is one of the more common ways in which the material is removed. Typically the energy of deformation for a ploughing process is defined as the product of polymer-yield-pressure and area of grooved-track. In the event of the metal sliding over the polymer, the polymeric material is conveyed right onto the counterface front. Therefore in a while the friction coefficient is effectively the contact between polymer-polymer interfaces. If one considers elastic deformation then it is quite important to talk about size, shape and distribution of the asperities. There are a number of factors that affect the friction of polymers such as sliding speed, sliding temperature, roughness-of-

counterface, applied load, contact pressure, material properties, humidity, surface wettability, and polymeric fatigue. [29]

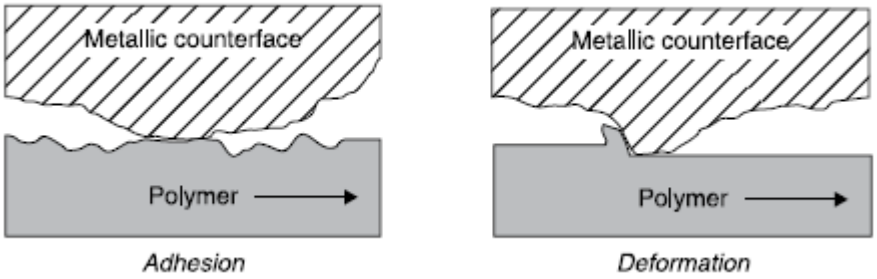

Figure 2.1. Friction Mechanism in Adhesion and Deformation [29]

As shown in the fig. 2.1, there may be two types of friction-mechanism generated. In the first case the interface medium has the polymeric-material and the metallic-counterface adhered to each other and results in material take-off or transfer from its original polymer as the faces slide against each other. In the second case the material forms a lump sticking onto the parent metal. It is imperative to understand friction and its characteristics in functional polymers before its application in real-time. If the friction coefficients tend to quite high it denotes a high probability of wear. If the wear rates are high then either the material properties could be controlled whilst processing or by the use of lubricants which could reduce the action of friction.

2.2 WEAR CHARACTERISTICS OF FUNCTIONAL POLYMERS

Wear is defined as the progressive substance-loss/degradation from the surface body under the action of mechanical, chemical or thermal influences. Recent upgrades and applications of functional polymers include biomaterials, gears, bearings etc. It is quite imperative to understand the contact conditions of polymers with counterface surfaces, usually made of steel, during its sliding test against each other. The other factors that affect the polymeric-wear are temperature, speed and applied load. The process of classification of wear is not an easy task in tribological testing as there are many types of wears. The major wears are abrasive, adhesive and surface fatigue and what's

interesting is that all may occur simultaneously or in other cases just permutations. In addition to these major wears there are also minor wears, both the categories being listed below [2, 29].

- Abrasive Wear
- Adhesive Wear
- Surface Fatigue
- Erosive Wear
- Corrosive Wear
- Fretting Wear

Abrasive wear is caused by asperities that are hard in nature, present on the counterface which interact with the rubbing surface of the polymer and ultimately unfasten material. In the wear process there may be chips or flecks produced as wear debris. The abrasive wear is directly proportional and dependent on the apex angle, the grit makes with the polymer surface and the shape of the abrasive points that move along the polymer surface. And also, it is inversely proportional to the product of nominal tensile breaking stress and elongation to break. The abrasive wear process typically involves both shear and plastic-deformation, see fig. 2.2. [29]

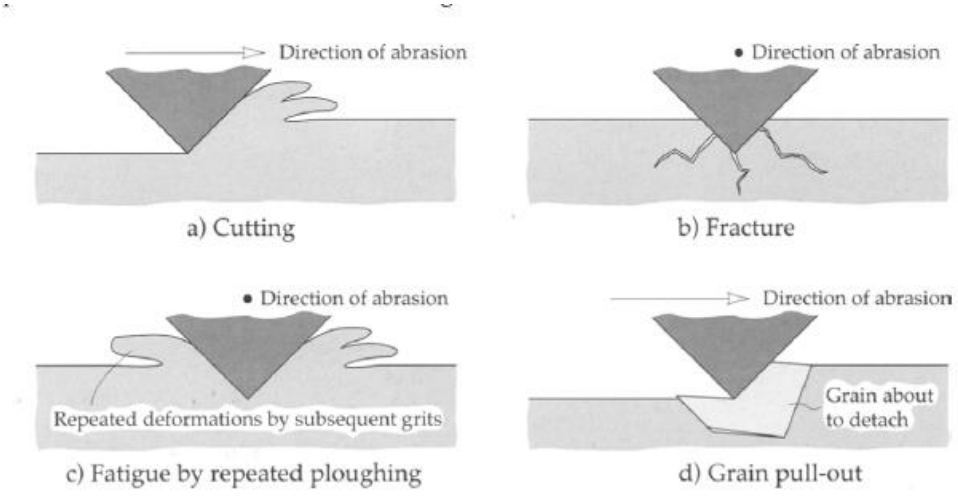

Figure 2.2. Mechanism of Abrasive Wear [2]

Abrasive wear that is produced due to counterface (dry steel) and polymer (polyamide 66) is depicted in fig. 2.3. The direction of rubbing can be observed using the slide-marks in contrast to the natural surface detail of the polymer. The run after a sliding distance of 80 km at magnification of 10x is depicted. The abrasive sliding marks depends on the surface topography of the polymer and

the hardness of the counterface. The direction of abrasion is also very important as various effects such as cutting, fracture, plough-fatigue or grain pull-out could occur. [2, 29]

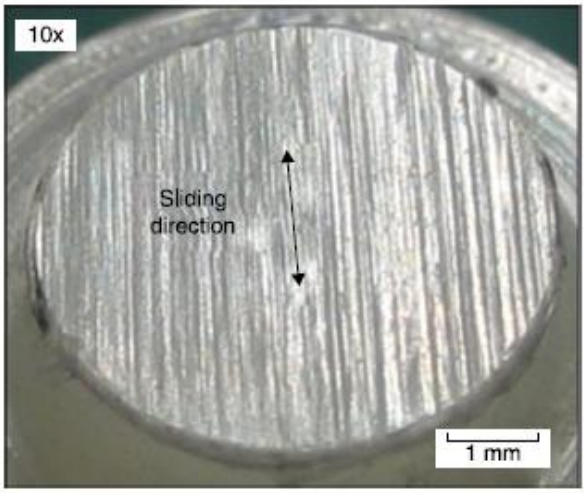

Figure 2.3. PA66 vs Dry Steel, 80 N, 80 km [29]

Adhesive wear, see fig. 2.4, is a common form of wear that is distinguished by large fluctuating friction-coefficients and high degree of wear rates. This typically arises from the shear parameters involved in the process of adhesive bonding. High local pressure is experienced between the polymeric surface- and the counterface resulting in formation of plastic deformation concluding an adhesive junction. The culmination of this exercise leads to junction-rupture. A thin film of soft-polymer is conveyed onto the hard mating surface followed by transfer-film buildup. [2, 29]

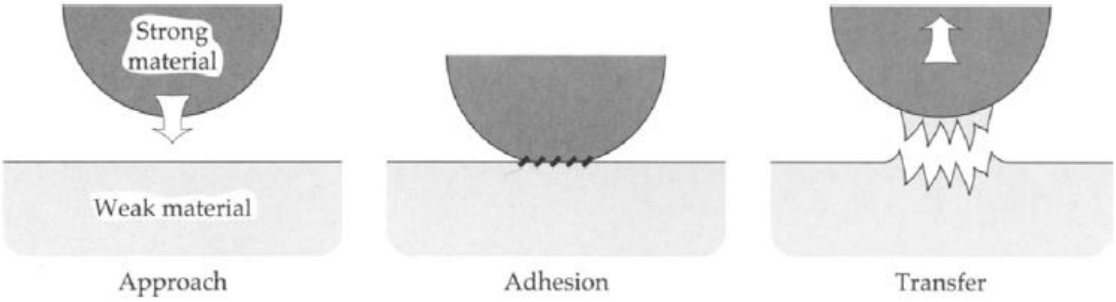

Figure 2.4. Mechanism of Adhesive Wear [2]

Thus the surface topography changes and a new equilibrium is reached. The friction coefficient changes during the running-in stage. The running-in stage is defined as the period in which the coefficient of friction varies significantly before steady state condition. Repetitive sliding of the polymer and the metallic counterface over each other results in the cohesion of parts of the polymer with the metallic counterface in contact.

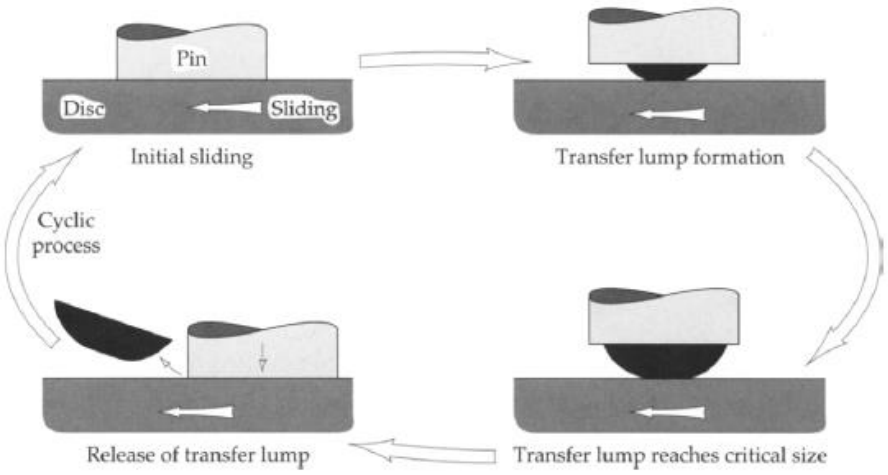

Figure 2.5. Mechanism under repetitive sliding [2]

One of the striking features in the adhesion wear is the formation of transfer film wherein a material is conveyed from one surface to the other before being ejected as a wear particle, see fig. 2.5. The formation and release of the transfer film happens in four stages. The first stage is wherein the process of initial sliding takes place, that is the surfaces rub against each other by virtue of sliding. In the second stage the transfer-lump is formed. In the tertiary stage the transfer-lump reaches a critical size and in the final stage the transfer-lump is released by sliding process. An example of polymer-transfer file, with constraints pertaining to polymer-polyamide with counterface-material steel has the following profile, see fig. 2.6. [29-32]

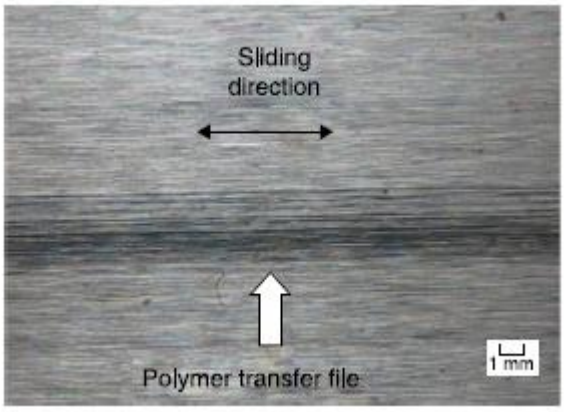

Figure 2.6. Steel counterface displaying transfer film of PA-20km-90N [29]

Surface fatigue has the definitions that tune to the polymer undergoing repeated stressing during rolling and sliding motion. This predominantly is noticed in almost all wear modes considering formidable friction. One can also notice the effect of surface fatigue at both rolling and reciprocal sliding. Thus loading and unloading can be observed on the polymeric-surface by the counterface-asperities.

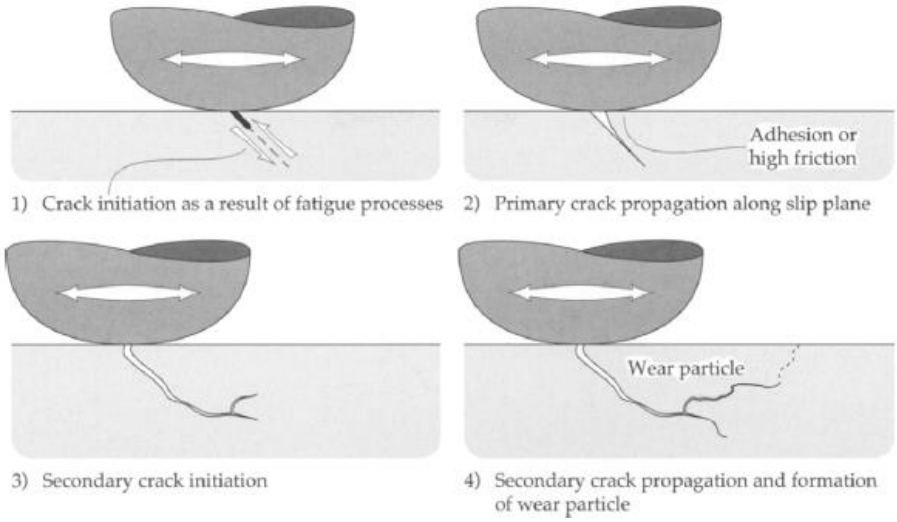

Figure 2.7. Mechanism of Surface Fatigue Wear [2]

This cyclic process, see fig. 2.7, results in subsurface crack initiation, further on leading to crack propagation and finally debris-spalling. Progressively, flaking-off of fragments becomes brisk or

prompt. The stress involved in surface fatigue process depends predominantly on the polymer's mechanical properties. The defects that cause this propagation may be listed as follows: [29, 33]

- Surface Marks, Dents
- Cracks, Pits and Voids
- Impurities
- Cavities

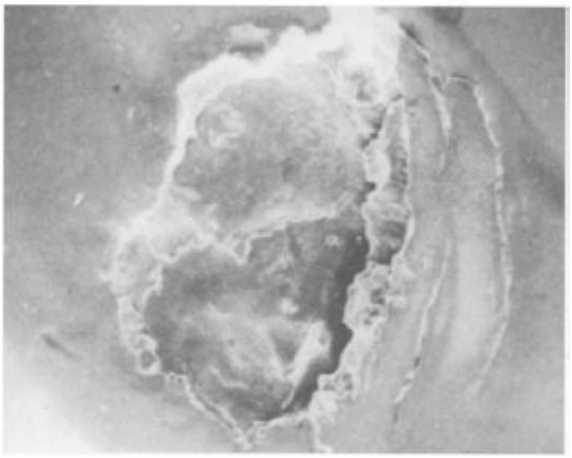

Figure 2.8. Surface initiated spalling - Surface Fatigue [2]

In this type of spalling as shown in fig. 2.8, the characterization is done by the distinctly produced pits. They can be either at surface level or sub-surface level. It can be observed that there is a superficial pit with multiple cracking in fig. 2.8. There is also flaking at particularly one portion of the pit. The surface initiated spall has its failures associated with reasons such as excessive surface roughness, billowing debris sizes and insufficient film thickness. One of the ways to avoid this kind of failures is to employ lubrication. This can reduce surface-dents and stress-concentrations which yield the very process of crack propagation.

Erosive wear occurs due to action of a liquid or a solid particles on an object. There are numerous examples of this, a few being wear of pump impellers in slurry systems, wear of gas turbine blades etc. Since the mechanical strength does not play a major role against wear resistance it is important to consider the material characteristics. [29]

Chemical wear also termed as corrosive wear comes into play when both corrosion and wear mechanism operate simultaneously in a chemical environment. An important criterion for this to

happen be that the worn volume should be substantial compared to the additive effects of each process taken singly. The corroded layer is then removed by abrasion wear by sliding process. [29]

Fretting wear occurs due to oscillatory motion of the surface in contact. This contact has constraints pertaining to small amplitudes and low speeds. In other words the polymer undergoes continuous vibration with either load acting or a load-independent condition. The accumulated debris remains in the interface and escalates the wear process by the virtue of a three-body abrasive wear process which is the interaction between the two objects of sliding and the wear debris. [29-33]

It is therefore important to understand the various wear mechanism that operate under the testing of functional polymers. If the type of wear is gauged, remedy or pre-requisite action can be taken to cause less material-wear. Either the properties of the material can be modified by addition of fillers or the processing conditions of the polymer can be transformed to rectify the impediment.

3 ANALYSIS OF TRIBOLOGICAL-TESTING METHODS

3.1 TRIBOLOGICAL TESTS-CONFIGURATION AND ANALYSIS

Friction and wear in polymers is quite a natural tendency and therefore it is important to estimate it using tribological methodologies. Wear as such is dependent on many factors such as sliding velocity, sliding media, counterface roughness and applied load. There is not a precise theoretical model for determining the wear phenomenon. Wear by definition is the progressive loss of material from the surface. Thus, the fundamental quantity for measuring wear is usually volume-loss however in some material studies mass-loss is also used. Typically the loss in dimension results in the proliferation of a clearance or contour-change. There are a variety of operational measures for determining the wear and some of them are vibrational level, crazing, lifetime, surface appearance and noise level. In order to study the wear in a pragmatic condition it is important to simulate it in a controlled environment. Therefore a number of factors such as measuring technique, sample preparation, data analysis, test apparatus (tribometer), data-recording etc. must be taken into consideration. There are a few points that have to be considered for a suitable wear test, they are: [29]

- Selected test should measure the intended properties.
- Surface roughness of rubbing faces should be identical or similar to actual applications.
- The range of loads and stresses should match the actual applications.
- Temperature, humidity, sliding media as in external conditions should simulate the real-time application.
- The test-duration and materials used, should be well defined.

There are different motions involved in the configurations such as sliding, reciprocation, rotation etc. In actual practice the motion in one type of wear test may be provide a better simulation of a real-time application. Since the use of polymers is found largely in sliding applications, the sliding wear tests with different test-configurations are employed to better gauge the tribological properties. The tribological tests also have standards such as the ASTM G99 or ASTM 133 but does not specify the values for the parameters such as test-rigs for accommodating polymer specimens and type of wear paths, but allows researchers to select it themselves and simulate the test for the application. Wear results are obtained by conducting tests that predefines the sliding distance, selected values of load

and speed. Wear vs Volume in some cases may be the output to analyze for different specimens with respect to varied testing conditions. Before the actual application there are simple test configurations that are quite useful in estimation of tribological properties. The simple tests have two categories of motion that are unidirectional sliding and reciprocating sliding. Under sliding wear tests we have the following configurations that define the tribological tests. [29-31]

Unidirectional Sliding

- Pin-on-Disc configuration
- Block-on-Ring configuration
- Pin-on-Drum configuration
- Ball-on-Disc configuration

In the case of unidirectional sliding application the Pin-on-Disc configuration has been put to practice most extensively. It has been commissioned in many applications to measure material wear and frictional properties at high temperatures and under lubrication & controlled atmospheres. The basic Pin-on-Disc configuration consists of pin-sliding against a rotating counterface (see, fig. 3.1). The configuration of the Pin-on-Disc apparatus consists of a pin that is loaded and sliding against a rotating disc. The motion is unidirectional and at constant speed. The test parameters are size and shape of pin, speed, load and material pairs. The schematic of the Pin-on-Disc configuration is as follows:

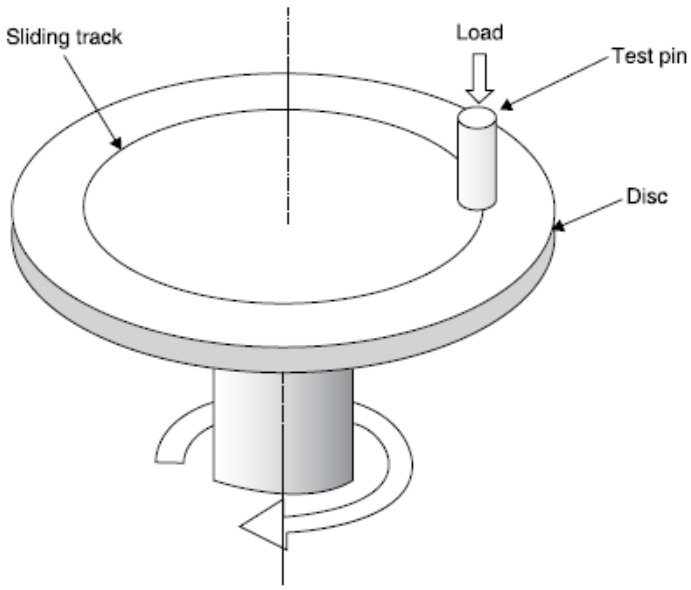

Figure 3.1. Schematic of Pin-on-Disc sliding wear test [29]

To estimate the contact pressure between the pin and the polymeric disc, it is given by the following equation by the Hertzian contact theory: [2]

$$P_{p-d} = \frac{W}{\pi k^2},$$

$$Where, P_{p-d}: Contact\ Pressure\ (Pa),\ W: Normal\ Load\ (N), k: Radius\ of\ the\ pin\ (m)$$

A. Golchin et al. [34] studied the influence of carbon based nano fillers incorporated into UHMWPE under water lubricated sliding contacts with a Pin-on-Disc configuration. The carbon based nano fillers used were multi-walled carbon nano tubes (MWCNT) and graphene oxide (GO). Research was done to study the influence and effects of (gamma)-irradiation and hygrothermal aging on the friction and wear response of the polymeric materials. Two carbon filled UHMWPE nano composites were synthesized along with virgin UHMWPE being taken as reference material. The polymer UHMWPE had grade GUR 1020 with average molecular weight, average particle size and density as 3.5 x 10^6 g/mol, 140 µm and 0.93 g/cc respectively.

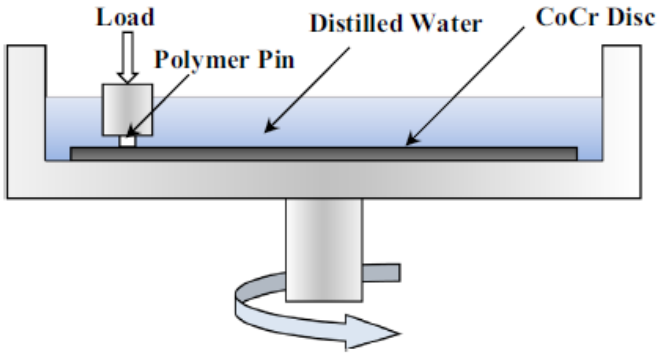

Figure 3.2. Schematic of test configuration [34]

Cubic polymer pins of dimensions 4 x 4 x 4 mm^3 were used. The tribological testing of the materials was carried out using a Pin-on-Disc tribometer, see fig. 3.2, on a CoCr disc test configuration (i.e. Co: 65.74 %, Cr: 27.11 %). The experiments were done at room temperature (21-25 °C), the load applied being 80 N and the contact pressure of 5 MPa. The sliding speed was a constant at 0.13 m/s also being the lowest rotational speed of the tribometer. The surface roughness of the discs were R_a = 0.7 µm.

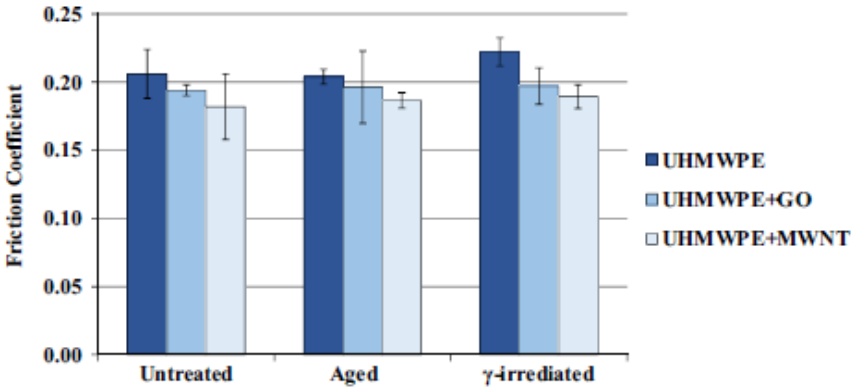

Figure 3.3. COF vs Treatment type [34]

The above fig.3.3, depicts the friction coefficient obtained for the different materials and its respective combinations & treatments. Generally, there was no predominant change in the friction coefficient observed upon aging and gamma-irradiation of the polymeric material. Regardless of the type of treatment that was employed, UHMWPE composites exhibited constantly, rather a low friction coefficient in relation to the unfilled polymer- UHMWPE. This is attributed to the boundary lubricating characteristics of GO and MWNT.

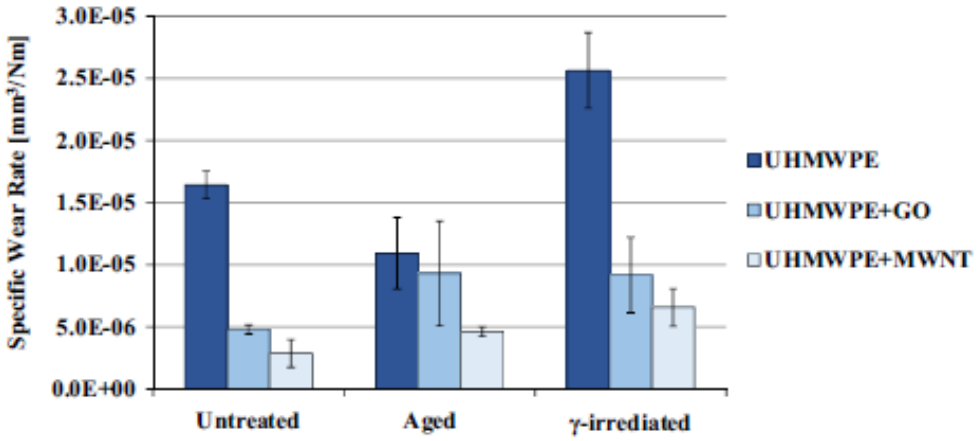

Figure 3.4. Specific Wear Rate vs Treatment type [34]

The study of steady-state wear rate for each material is defined by the above histogram as shown in the fig. 3.4. Aging of polymers seemed to decrease the specific wear rate of the pure-polymer in general. However the case with polymer composites was quite different. Authors suggest that this is because of the degradation of the filler/matrix interface in the presence of moisture and heat. Gamma-irradiation in any case did not improve the wear resistance. However the mean wear rate was lower for the composites in comparison to the unfilled UHMWPE. Authors point out that the incorporation of GO or MWNT can lead to changes in the mechanical, thermal and structural characteristics of UHMWPE and thus influence wear and friction rates. The improved tribological behavior of UHMWPE upon subsuming MWNT/GO into it, is attributed to the action of nano-fillers in water lubricated sliding contact. Thus the Pin-on-Disc configuration was observed to be a simple and convenient method of testing polymers.

In modelling some aspects of sliding applications, Block-on-Ring (see, fig. 3.5a), ASTM G137, Pin-on-Drum (see, fig. 3.5b), ASTM G65 and Ball-on-Disc configuration (see, fig. 3.6) are used.

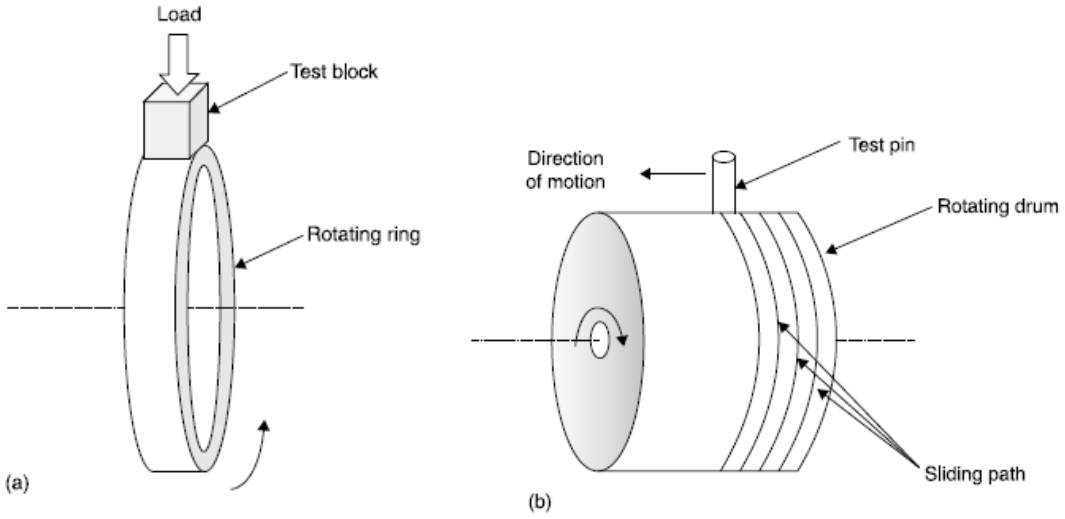

Figure 3.5. Schematic of (a) Block-on-Ring (b) Pin-on-Drum [29]

The ASTM standards gauge the amount of wear by virtue of linear-dimension measurement before and after operation. This testing is done by weighing specimens for the difference, which indicates the weight/mass loss. In actual practice, linear measures are taken into account since mass loss ordinarily is difficult to measure accurately. The material pair that undergoes the test would determine if both the disk (or drum) and pin (or ball) or one of them in the subset would be predominantly worn.

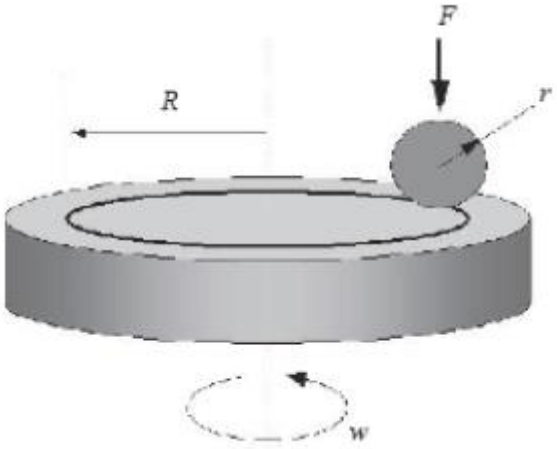

Figure 3.6. Schematic of Ball-on-Disc setup [35]

To estimate the contact pressure between the ball and the polymeric disc, it is given by the following equation from the Hertzian contact theory. By employing these equations the contact pressure can be estimated which is directly dependent on the normal load. The normal load can be varied using different mass-standards. [2]

$$P_{b-d} = \frac{3F}{2\pi a^2}$$

$$a = \left(\frac{3WR'}{E'}\right)^{1/3}$$

$$R' = \frac{r}{2}$$

$$\frac{1}{E'} = \frac{1}{2}\left(\frac{1-\vartheta_a{}^2}{E_A} + \frac{1-\vartheta_b{}^2}{E_B}\right)$$

$Where, P_{b-d}: Contact\ Pressure\ (Pa),\quad F: Normal\ load\ (N),\quad R': Reduced\ radius\ (m)$

$E': Reduced\ Young's\ Modulus\ (Pa),\quad \vartheta_a: Poissons\ ratio\ of\ ball,\quad \vartheta_b: Poissons\ ratio\ of\ disc$

$r: Radius\ of\ ball\ (m)$

The other type of sliding is reciprocating sliding and subcategories the following:

Reciprocating Sliding

- Pin-on-Plate configuration
- Ball-on-Plate configuration

The Pin-on-Plate is a reciprocating (sliding) motion wear-test to determine friction and wear. This test method simulates the geometry and motions that come about in many rubbing components. Here the normal operation involves periodic reversal in the sliding direction. The data and result yielded from this type of motion (reciprocating sliding) varies from the process of unidirectional sliding. Different material combinations may yield different results. Typically, the rubbing mode is simulated by a radius-tipped or a flat-ended test pin pressed against a flat counterpart which moves back and forth in reciprocating motion, (see fig. 3.7). A feature of the change in motional-direction depicts that there are portions for acceleration and deceleration. The sliding velocity varies with the type of test rig used and drive mechanism. Fundamentally, the reciprocating sliding test can be used to simulate conditions that host fretting mechanisms. Other critical imperatives here are frequency, contact pressure and amplitude.

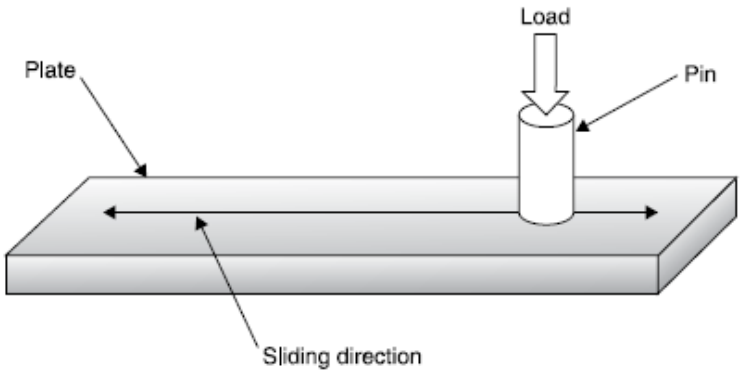

Figure 3.7. Schematic of Pin-on-Plate test [29]

P.L. Menez et al. [36] studied the tribological properties of UHMWPE pins rubbed against steel plates by an inclined Pin-on-Plate sliding tester. Tribological properties such as coefficient of friction and transfer film formation were observed in this study. The roughness features and fracture features were quantified using optical profilometer and SEM respectively. In this study, UHMWPE (grade GUR 415) as polymer in the shape of a pin with dimensions, 10 mm in length and 3 mm in diameter were used. The corresponding tip radius was 1.5 mm. The counterpart steel plates were materialized of 080 M40 steel material. The dimensions of the plate were 28 mm x 20 mm x 10 mm.

In this study the surface textures of the steel plates were categorized into three types which were unidirectional (grinded the steel plate in a unidirectional direction with emery paper), 8-ground (generated in a shape of an 8 with emery paper) and random (wet polishing technique, which involved steel plate to be rubbed against a pad of standard metallographic disc of a polishing machine). Further on there were four surface texture parameters in actual study since the unidirectional surface texture were further subdivided into two types; pin-slid perpendicular to the direction of unidirectional grinding marks (UPD), pin-slid parallel to the direction of the grinding marks (UPL), 8-ground and random-surface topography orientation.

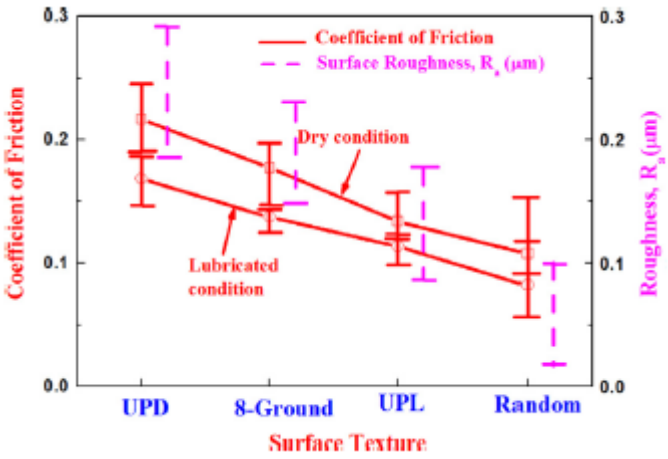

Figure 3.8. Surface Texture vs COF and Roughness [36]

The tests were conducted both for dry and wet lubrication conditions. The inclined Pin-on-Plate slide tester had an angle of 1°.The normal load ranged from 1 N to 70 N for a wear track length defined to be at 10 mm. The sliding velocity during the test was 2mm/s. The lubricant used was an SAE 40 engine oil with volume of 0.05 ml smeared up on the surface of the steel plate. For the two set of tests as shown in fig. 3.8 (dry and wet lubrication), the coefficient of friction dropped down from UPD, subsequently to 8-ground, to UPL and to Random orientation. The unidirectional sliding perpendicular to the grinding marks yielded the highest coefficient of friction for conditions of both types of lubrication. The authors put forth that COF depends upon the surface texture considerably. The authors suggest that transfer film formation depends on the COF which in turn is banked on surface roughness and texture of material. The Pin-on-Plate configuration was observed to less simple when compared to the Pin-on-Disc configuration.

A. Ruggiero et al. [37] researched the friction and wear behavior of UHMWPE slid against two materials namely AISI420C austenitic stainless steel and $TiAl_6V_4$ under condition of dry and wet lubrication. The testing conditions were studied with a reciprocating Pin-on-Plate tribometer, see fig.3.9. The tests were carried out by varying the frequency of alternate motion of the pin and the normal applied load. The lubricant used was sodium hyaluronate. By the employment of an electronic precision balance the loss of wear mass was estimated.

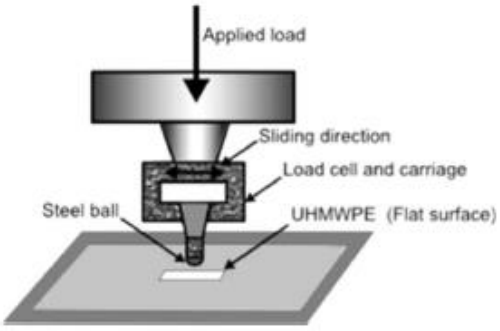

Figure 3.9. Schematic of reciprocating Pin-on-Plate tribometer [37]

The machine load ranged from 1 N to 20 N. The operating frequency range was from 0.1 Hz to 35 Hz. The material used UHMWPE (GUR 1050) was cut to a dimension of 5 x 5 x 5 mm^3. The austenitic stainless steel AISI 420C pin and $TiAl_6V_4$ had a radius of 3 mm and was spherical in shape.

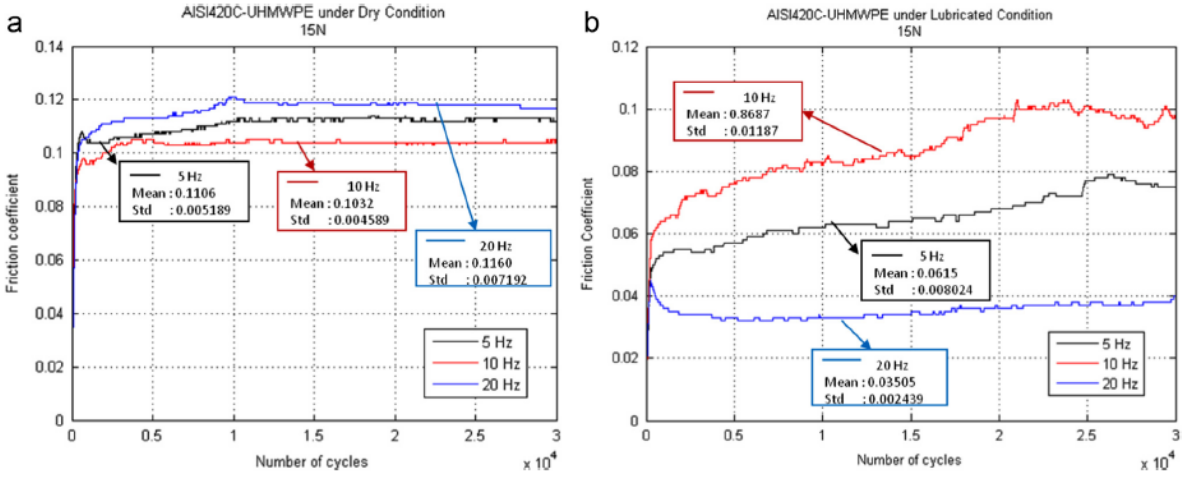

Figure 3.10. The evolution of the friction coefficient for normal load of 15 N: (a) under dry conditions and (b) under lubricated conditions in AISI420C–UHMWPE contact [37]

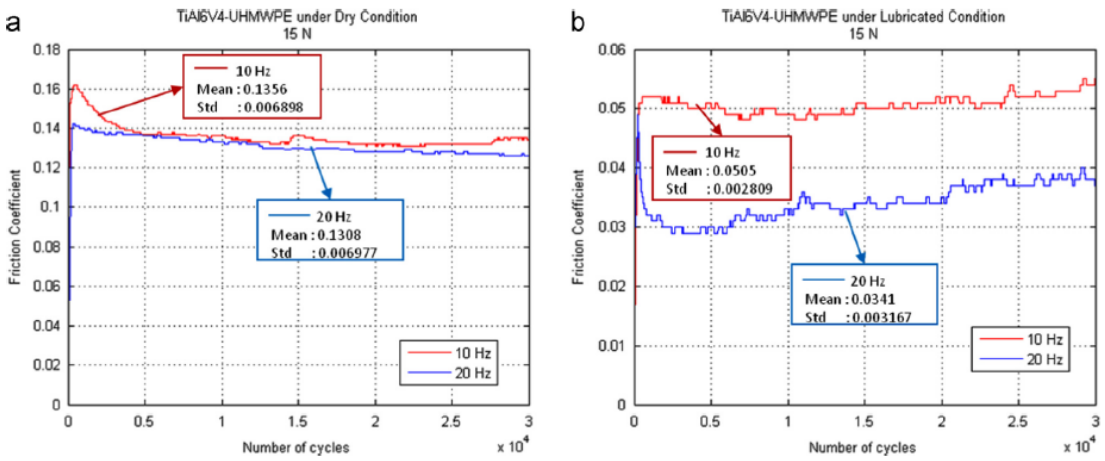

Figure 3.11. The evolution of the friction coefficient for normal load of 15 N: (a) under dry conditions and (b) under lubricated conditions in $TiAl_6V_4$–UHMWPE contact [37]

The tests were performed at dry and wet lubricated conditions. The normal contact loads applied were 10N, 15N (see, fig. 3.10, 3.11) and 20N for UHMWPE/AISI 420C steel and 15N, 20N for UHMWPE/$TiAl_6V_4$ alloy. It can be observed that by the addition of a lubricant, the friction coefficient reduced quite well. On the overall, the friction and wear characteristics are summarized in fig. 3.12.

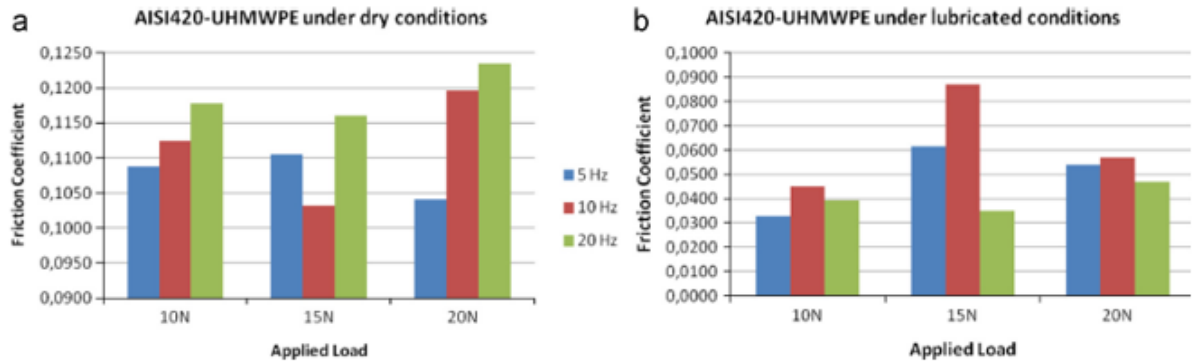

Figure 3.12. Average Values of COF for AISI 420C - UHMWPE under (a) dry conditions (b) lubricated conditions [37]

So as observed from fig. 3.12a, above, it can be noticed with frequency the friction coefficient typically increases (dry condition). But there were exceptions, as in fig. 3.12a, the load 15 N with frequency 10 Hz had a different trend because the metal-pin that rubs against the polymer- UHMWPE operated under self-lubricated conditions as the authors point out. In fig. 3.12b with the introduction of a lubricant as hyaluronic acid, the relation between frequency and load is not well defined and the

friction coefficient decreases. As the frequency increases from 5 to 10 Hz with load the friction coefficient increases but at 20 Hz there is a steep drop and this is probably due to the nature of hyaluronic acid used as lubricant that is quite viscous but at high speeds could depict distinction lubricative conditions such as mixed/hydrodynamic type as the authors suggest.

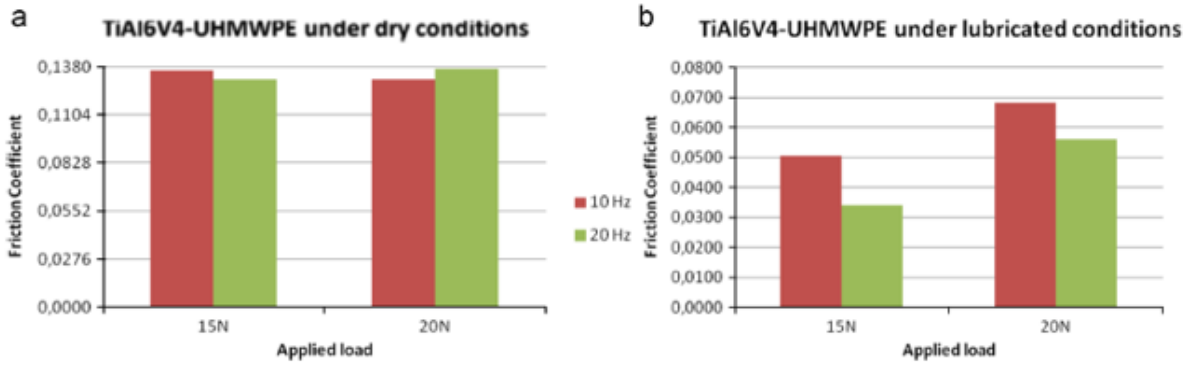

Figure 3.13. Average values of COF for $TiAl_6V_4$- UHMWPE: (a) dry conditions (b) lubricated conditions [37]

For the titanium alloy as shown in fig. 3.13 with increase in frequency and also with the addition of a lubricant, the friction coefficient decreases. But there is a distinction except with the 20 N, see fig. 3.13a, wherein the friction coefficient increases which is one anomaly with regard to the above theory.

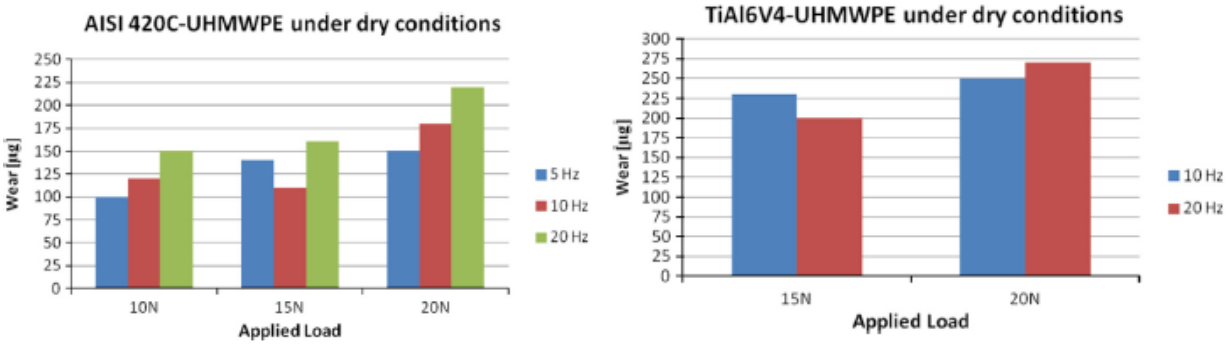

Figure 3.14. Wear rate vs Load for AISI 420C and $TiAl_6V_4$ with polymer- UHMWPE under dry conditions. [37]

Now relating to the concept of wear rate (dry conditions), the characteristics of the histogram (see, fig. 3.14) are quite similar to the friction characteristics with the exception at 15N load at 10Hz frequency as previously discussed although the theory assumed is that with increase in loads and

frequency, the friction coefficient increases. The results thus show that the AISI420C austenitic stainless steel working against UHMWPE, gives better values that $TiAl_6V_4$/UHMWPE in friction and wear performances in dry conditions. In both cases, friction decreases because of the presence of UHMWPE that aids in the formation of a lubricating film in the contact zone thereby promoting self-lubrication at the contact. It is observed that with the addition of the lubricant, the friction coefficient and wear volume decreased due to different lubricative mechanisms that require further investigation as the authors expound.

In the research work done by M. Guezmil et al. [38] UHMWPE was tested against M30NW stainless steel on a reciprocating Pin-on-Disc tribometer which was essentially a Pin-on-Plate configuration due to the reciprocating motion of the base. The testing was done under both dry and lubricated conditions. Here saline solution with 0.9 % sodium chloride in deionized water, sesame oil and nigella sativa oil were employed for bio-lubrication. The aim was to study the wear volume and friction coefficient of UHMWPE.

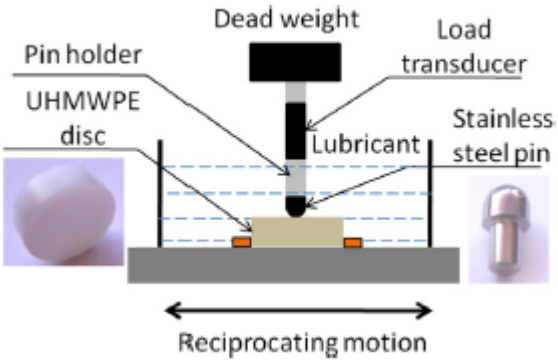

Figure 3.15. Schematic of reciprocating Pin-on-Disc tribometer with UHMWPE against Stainless Steel [38]

The setup had a M30NW stainless steel pin that was hemispherical in shape. The diameter of the pin was 10 mm. The discs of the polymer-UHMWPE were machined as to assume a cylindrical shape with diameter of 30 mm and thickness of 10 mm. The wear tests were conducted at room temperature and the samples were polished to 0.31 ± 0.05 µm. The roughness of the stainless steel pins were 0.06 ± 0.01 µm. The normal load applied during the test of friction was set to be at 20 N, see fig. 3.15.

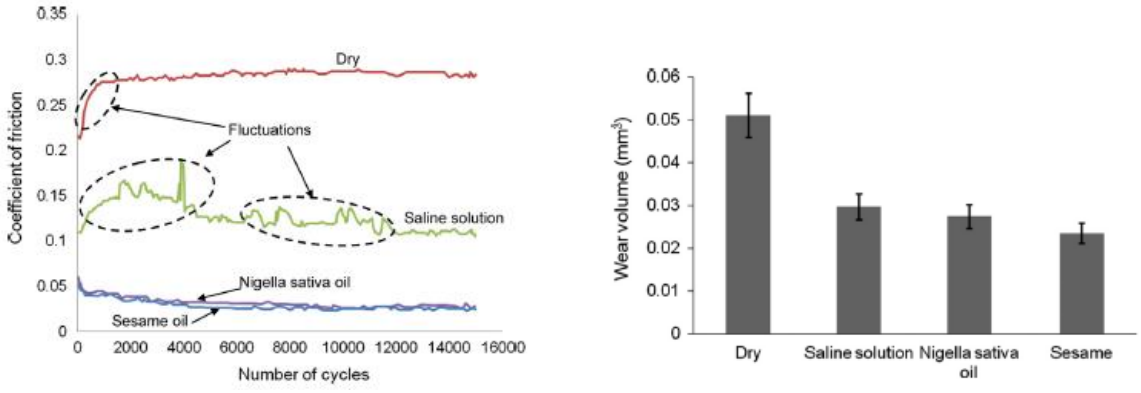

Figure 3.16. Fig. (a) COF vs Number of Cycles (b) Wear Volume vs Lubricant-type [38]

It was observed that the performance of the nigella-sativa oil and sesame oil as natural-lubricants were quite formidable as shown in fig. 3.16. In terms of both the wear rate and friction coefficient the performance of nigella-sativa oil and sesame oil outclassed the saline solution and the case of dry lubrication. Morphological and chemical tests and analysis also reveal that the type of wear between mechanism in dry conditions, saline solution (NaCl 0.9 %) and oil-lubricated conditions were adhesive-abrasive, adhesive-oxidative and adhesive respectively. The authors suggest that the results attribute to the natural composition of the oil and the adsorption property of the M30NW stainless steel. In other words the low coefficient of friction and wear volume were attributed to adsorption of fatty acids on the stainless steel surface with the formation of carboxylate complex soap. The tribological behavioral difference between oils nigella-sativa and sesame, was closely attributed to unsaturated fatty acid proportions.

A. Ruggiero et al. [39] studied the friction and wear behavior of polymer- UHMWPE sliding against three counterfaces which were $TiAl_6V_4$ alloy, AISI316L steel and Al_20_3 ceramic, under dry and lubricated conditions. The lubricant used was a fluid containing sodium-hyaluronate. The configuration of the Tribometer had a Pin-on-Plate setup. The worn surfaces had been examined using 3D confocal microscopy. Now considering the result plots for UHMWPE / $TiAl_6V_4$ (see, fig. 3.17a, 3.17b), UHMWPE/AISI316L (fig. 3.18a, 3.18b) and UHMWPE/Al_20_3 system (fig. 3.19a, 3.19b):

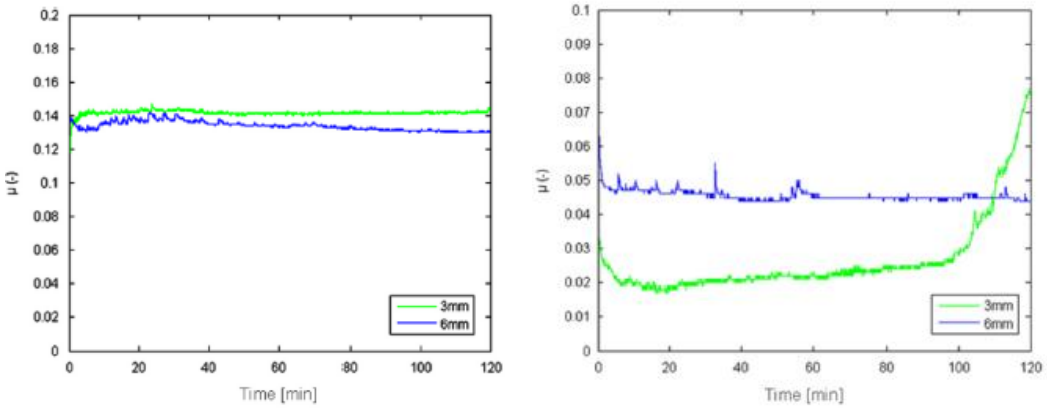

Figure 3.17. Fig. (a) Dry and (b) Lubricated conditions for UHMWPE/$TiAl_6V_4$ with different pin diameters, COF vs Time [39]

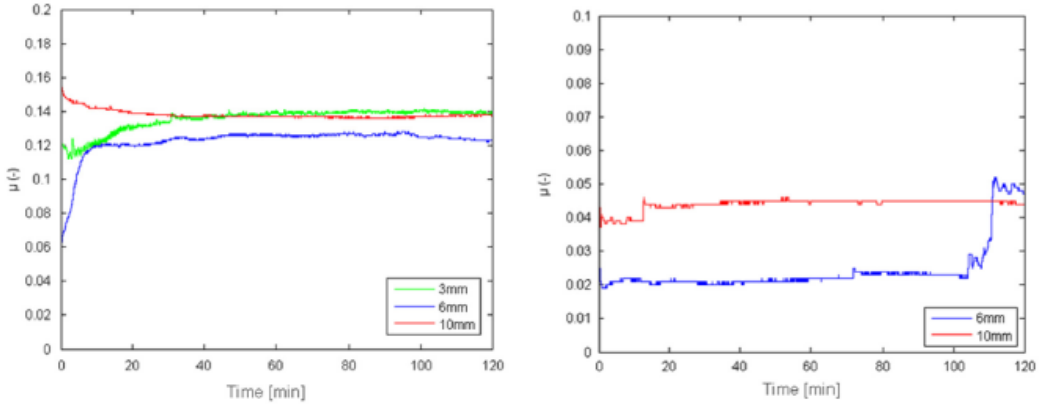

Figure 3.18. Fig. (a) Dry and (b) Lubricated conditions for UHMWPE/AISI316L steel with different pin diameters, COF vs Time [39]

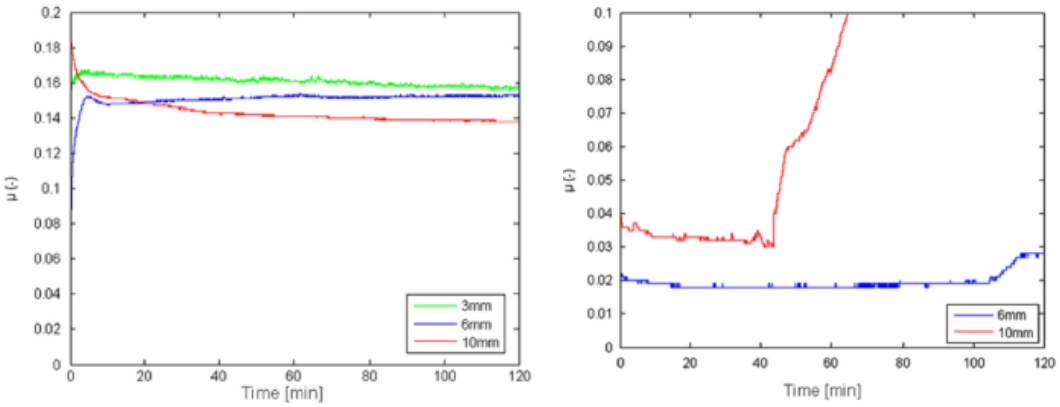

Figure 3.19. Fig. (a) Dry and (b) Lubricated conditions for UHMWPE/Al_20_3 ceramic with different pin diameters, COF vs Time [39]

For dry lubricated conditions (see, fig. 3.17a, fig. 3.18a, fig. 3.19a) that initially the coefficient of friction was low, proliferated rapidly and then stabilized. No interrelation could be derived between pin diameters and friction coefficients. The fluctuations observed in the dry test heightened during the first 20 mins of the test. The dry lubrication induced geometric and chemical modifications on both the pin and the polymer. The maximum value of coefficient of friction was observed for the system UHMWPE/Al_20_3 ceramic.

In wet lubrication (see, fig. 3.17b, fig. 3.18b, fig. 3.19b) it could be noted that the introduction of lubricant fluid decreases the value of friction coefficient. It was also observed that the initial transient time expires in a span of 10 mins as opposed to the 20 mins in the previous case of dry lubrication. The viscosity of the lubricant when applied to a load-conditions and defined-speeds might give yield lubrication mechanisms such as boundary or transient type lubrication. Authors also suggest that the primary contrast between both the cases (dry, wet) of lubrication was the shape of the cycles. Additionally in the case of dry friction the friction-force evolution during sliding was milder and regular whereas in the case of wet lubricative conditions was more sharp and highly oscillatory. This indicates a sense of unstable boundary lubrication with the need for further research.

In the research work done by J. Huang et al. [40] one of the objectives was to analyze and investigate the tribological behavior and wear of UHMWPE infiltrated with alendronate sodium (ALN), a drug used in treatment of osterolysis. Alendronate sodium was dissolved in a 220 mL of deionized water-ethanol mixture into which 80 g of UHMPWE powder of average molecular weight $5 \pm 0.5 \times 10^6$ g/mol. The mixture was stirred at room temperature and dried at 40 °C in an air oven. The dried UHMWPE-ALN (1 wt. %) powder was hot pressed at a temperature at 180 °C and 15 MPa. A computerized reciprocating Ball-on-Plate sliding wear equipment was used, see fig. 3.20.

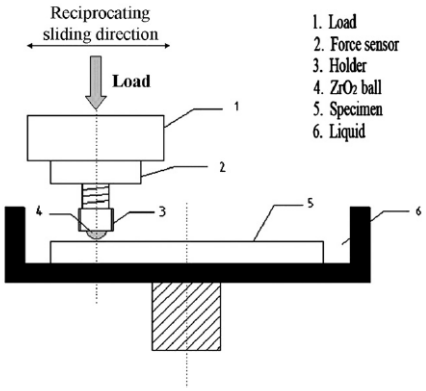

Figure 3.20. Schematic diagram of the computerized reciprocating ball-on-plate sliding wear apparatus [40]

UHMWPE-ALN and UHMWPE were made into blocks of dimensions 50 mm x 12.5 mm x 8 mm which was then ultrasonically cleaned in ethanol and air dried. The average roughness of the samples UHMWPE-ALN and UHMWPE were 0.18 ± 0.009 µm and 0.25 ± 0.008 µm respectively. A $Zr0_2$ ball of diameter 9.8 mm and R_a= 0.02 µm was pressed against the sample. The constant loads were 10 N, 30 N and 50 N. The linear velocity and frequency recorded was 30 mm/s and 3 Hz respectively.

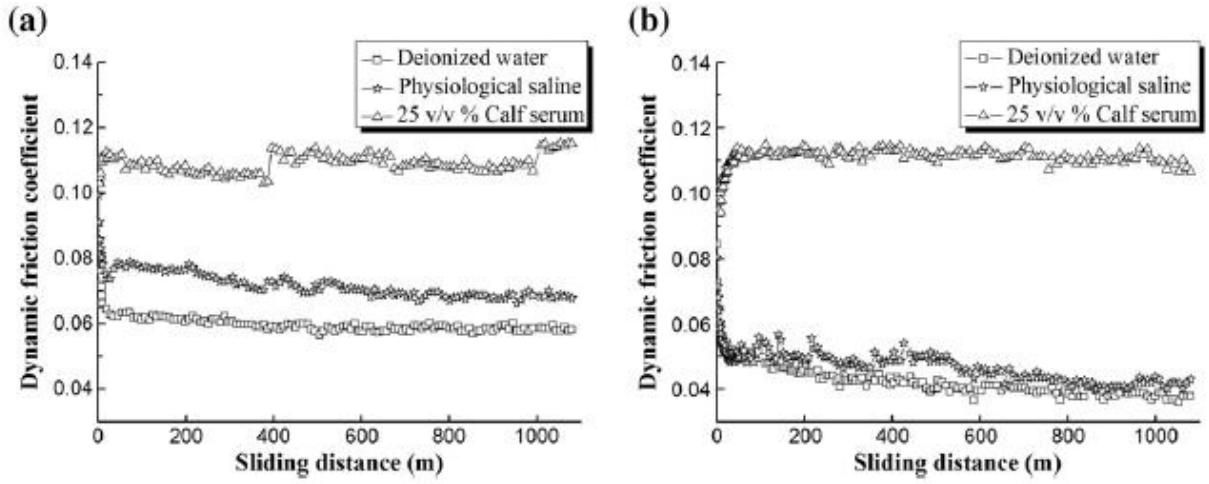

Figure 3.21. Variation of COF (a) UHMWPE- ALN (b) UHMWPE with sliding distance at the normal load of 30 N under deionized water, physiological saline and 25 v/v % calf serum conditions [40]

Dynamic friction coefficient variations of UHMWPE-ALN and UHMWPE, under a normal load of 30 N are depicted in the fig. 3.21. The coefficient of friction of UHMWPE were observed to be lower than that of UHMWPE-ALN in deionized water and physiological saline. The friction coefficient of UHMWPE-ALN and UHMWPE were found to be similar under conditions of 25 v/v % calf serum. In the case of deionized water and physiological saline, it followed a two-stage pattern, which was an initial drastic increase followed by slow decrease in friction coefficient. Now taking into consideration specific wear characteristics, the following was observed in fig. 3.22.

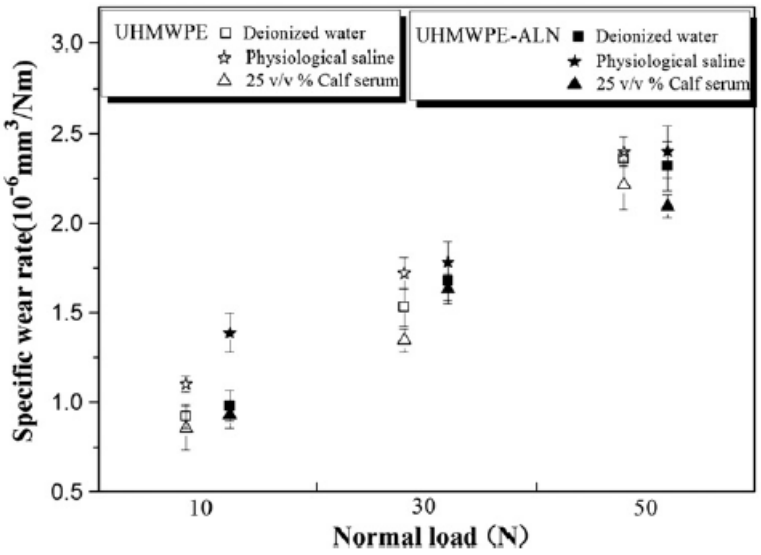

Figure 3.22. Variation of Specific Wear Rates of UHMWPE-ALN and UHMWPE with different normal loads and lubrication conditions [40]

The specific wear rates of UHMWPE-ALN and UHMWPE were highest in physiological saline whereas it was the least in the case of 25 v/v % calf serum. At 50 N in 25 v/v % calf serum there was significant difference in wear characteristics of UHWPE-ALN and UHMWPE, the former being lower. The specific rates of UHMWPE-ALN and UHMWPE increased with increase in normal loads consistent with wear-volume loss as authors expound. It was also observed that the main wear mechanism in the case of UHMWPE-ALN and UHMWPE in deionized water was abrasive. The wear mechanism in the case of UHMWPE-ALN and UHMWPE in physiological saline was micro-fatigue and abrasive respectively. In the case of 25 v/v % calf serum, the materials UHMWPE-ALN and UHMWPE exhibited abrasive wear with plastic deformation.

3.2 SUMMARY OF TRIBOLOGICAL TESTING

A brief summary of the various friction coefficients that had been yielded when polymer-UHMWPE was subjected to various counterfaces has been recorded in the table 3.1. The highest COF's were observed for a combination of UHMWPE/M30NW Stainless Steel (0.225 – 0.275). The least friction coefficient was exhibited by the UHMWPE/$Zr0_2$ (0.04 – 0.12).The values of these observations are used to compare with the experimental values in this work.

Table 3.1. Technical Summary

Polymeric Type	Coefficient of Friction	Type of Configuration
UHMWPE/CoCr	0.185 - 0.210	Pin-on-Disc
UHMWPE/Steel	0.113 - 0. 213	Pin-on-Plate
UHMWPE/AISI420C Steel	0.103 – 0.123	Pin-on-Plate
UHMWPE/$TiAl_6V_4$ Alloy	~0.138	Pin-on-Plate
UHMWPE/M30NW Stainless steel	0.225 - 0.275	Pin-on-Plate/Disc
UHMWPE/$TiAl_6V_4$ Alloy	0.134 - 0.142	Pin-on-Plate
UHMWPE/AISI316L Steel	0.125 - 0.138	Pin-on-Plate
UHMWPE/Al_20_3 Ceramic	0.141 - 0.161	Pin-on-Plate
UHMWPE/$Zr0_2$	0.04 - 0.12	Ball-on-Plate

There have a variety of tests that have been used by different authors used but the most basic test that is used in friction and wear estimation is the Pin-on-Disc method. This is a very simple test which simulates to a justifiable extent the actual working condition though not exactly. All the testing methods provides just a basic analogy to analyze friction and wear, but to gauge the veritable values, the applications have to be made into actual shapes and then tested. A polymeric gear test rig is an example. Sometimes the values of friction and wear seem unreal with the Pin-on-Disc testing which in practice may not be pragmatic. Thus the transition to Ball-on-Disc configuration or other configurations is done to gauge friction and wear characteristics, if the former methodology fails. The important parameters that define the tribological machines are normal load, sliding speed, sliding distance and contact pressure.

4 RESULTS OF EXPERIMENTAL TESTING

4.1 PRELIMINARY TESTING

4.1.1 Material Properties

The material that was used in this experimental work was polymer- UHMWPE (Ultra-High Molecular-Weight Polyethylene). Its key features and properties are defined in the following table 4.1.

Table 4.1. Properties of polymer-UHMWPE

Property	Value
Density	0.93 g/cc
Molecular weight	5 x 10^6 g/mol
Tensile Modulus	600 MPa
Yield Stress	17 MPa
Hardness	64 Shore D
Melting Temperature	130-135 °C
Thermal Conductivity	0.4 W/mK
Poisson's Ratio	0.4

The samples were cuboidal in shape. An illustration of the UHMWPE sample with dimensions is depicted in fig. 4.1. There were four samples with final processing conditions as follows; Sample1 (Standard cooling to room temperature), Sample2 (Prolonged cooling to room temperature), Sample3 (Standard cooling down in vacuum) and Sample4 (Prolonged cooling down in vacuum), see table 4.2. The desideratum was to gauge the ideal sample out of the lot in terms of friction coefficient and wear-resistance. In order to define this, there were preliminary tests that were conducted for tribological optimization.

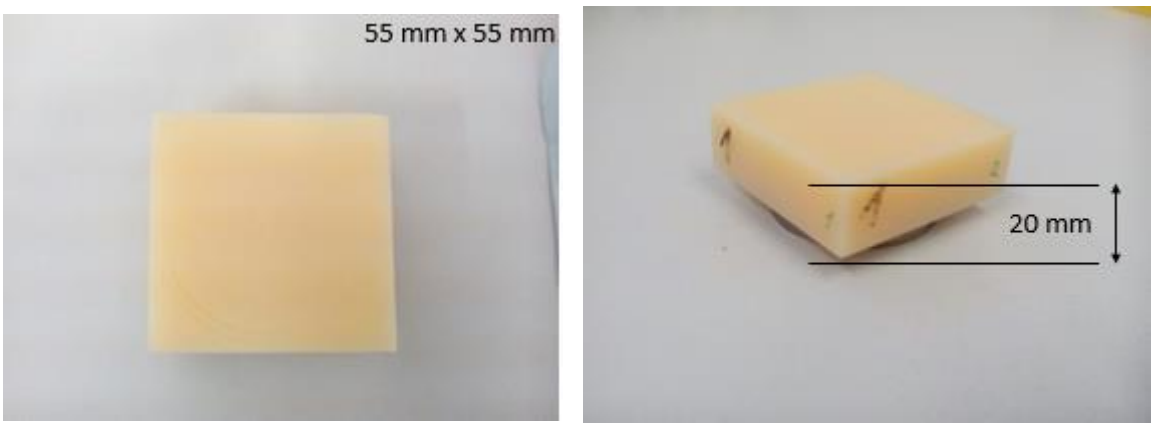

Figure 4.1. UHMWPE Sample

Table 4.2. Final-Processing Conditions of Samples

UHMWPE Sample No.	Final-Processing (Cooling-Down) Conditions
1	Standard Cooling-Down to Room Temperature
2	Prolonged Cooling-Down (14 hr) to Room Temperature
3	Standard Cooling-Down in Vacuum
4	Prolonged Cooling-Down (14 hr) in Vacuum

Polymer-UHMWPE has the properties of low friction, high abrasion resistance, wear and corrosion resistance. Its applications in general tend to be more in the sectors relating to mechanical engineering, food processing industry, bottling industry etc. Bearings are a major application. Specific applications include gear wheels, belts, bushes, sprockets, transport pallets, guide rails and wheels etc.

4.1.2 Equipment of Experiment

For the process of tribological optimization of the samples the Tribo-equipment that were used are an Automatic Polisher, Tribometer, Optical Microscope and a Profilometer. The Struers-Rotopol Automatic Polisher (see, fig. 4.2) was used to surface finish the polymer to a value of surface roughness, $R_a = 0.3 \pm 0.05$ µm.

Figure 4.2. Struers-Rotopol Automatic-Polisher [42]

The CSEM, Tribometer, (see fig. 4.3) was used for friction and wear measurement (Pin/Ball configuration). This machine had a unidirectional sliding motion with load application ranging from 1 N to 30 N. The sliding speed varied from 0.1 x 10^{-4} to 2 m/s. The polymer-placement module was cylindrical in shape with hexagonal cross sections. The values of Young's Modulus and Poisson's ratio for the steel Pin/Ball were 210 GPa and 0.3 respectively.

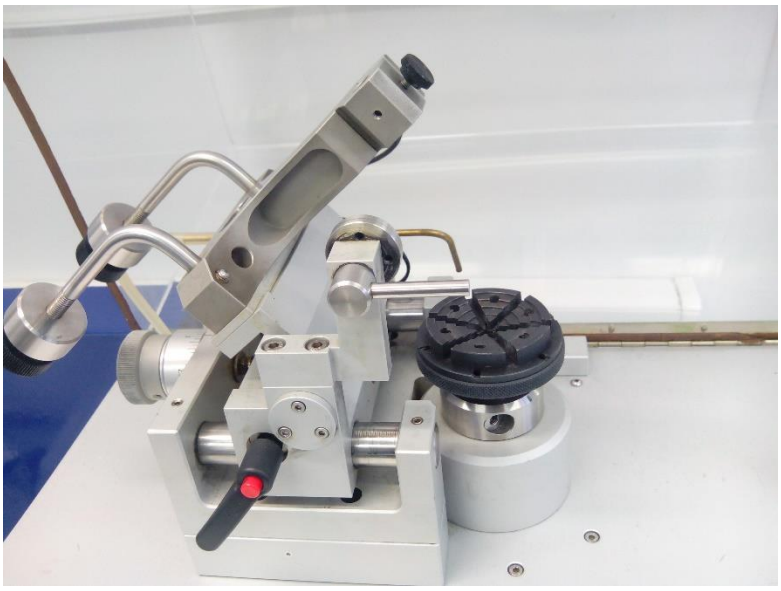

Figure 4.3. Tribometer- CSEM Instrument [42]

The instrument used for the purpose of wear-scar imaging in tribological-optimization was a 3D-optical microscope-Bruker-ContourGT-K0, see fig.4.4. The specifications relating to this instrument are the following; the operation mode had a white/green light interferometry with a scanning range of 30 mm x 30 mm in the abscissa-ordinate axis. The lateral resolution was 40 nm and the vertical resolution was 0.1 nm. The inbuilt equipment analysis involved both 2D & 3D frames in the measurement of surface topography, roughness parameter and wear volumes.

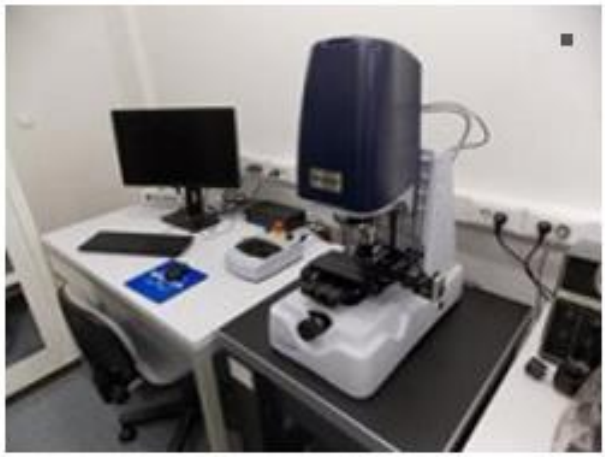

Figure 4.4.3D-Optical Microscope-Bruker-ContourGT-K0 [42]

The HOMMEL profilometer, see fig.4.5, had the value of surface roughness, R_a minimum rated at 10 nm. The instrument had a configuration with a stylus-tip contact. Here in this case polymer-UHMWPE was gauged for wear-scar depth measurements for initial tribological-optimization conditions. Three profilometer length-standards defined in this machine were as follows:

- 0.48 mm
- 1.5 mm
- 4.8 mm.

The profilometer had an integrated printer capable of proofing the wear plot for the wear-depth dimensions. This was exclusively used for preliminary testing (tribological optimization) of the UHMWPE samples.

Figure 4.5. HOMMEL Profilometer [42]

4.1.3 Testing Methodology

The objective basically was to measure and analyze friction and wear characteristics in the four different set of samples (see, Table 4.2) subject to varied final processing conditions. The algorithm (see, fig. 4.6) involving the preliminary testing which is followed by the secondary testing is depicted below. The primary step was to choose a random sample out of the four upon which tribological optimization in terms of load, sliding speed, sliding distance etc. was done. The succeeding step involved the extension of the tribologically-optimized conditions (secondary testing) to the other samples to analyze both friction and wear characteristics which is categorized under secondary testing procedures.

- Initial Friction and Wear Testing of Random Sample (Tribological Optimization - Preliminary Testing)
- Extension of Optimized Parameters to testing of Friction and Wear Characteristics (Secondary Testing)
- Analysis of best-fit sample.

Figure 4.6. Testing Methodology

There were a set of six steps that characterized the tribological-optimization of random sample (taken as Sample2) as described in table 4.3. In order to test the samples there were four spot-

references, see fig. 4.7, on the polymer depicting the wear-scar sides to be measured on the polymer due to the action of the steel pin on the polymeric disc. This was to understand the wear-scar depth variations on the four ends. They were numbered from 1 to 4 and in the secondary testing, detailed analysis of the wear-scar depth is done.

To find the superlative tribological-optimization condition there were a list of parameters that were employed in the tribometer; vertical load, linear speed, sliding distance, acquisition radius and type of configuration (Pin-on-Disc/ Ball-on-Disc) and contact pressure.

- The vertical load was defined by the mass standard. Linear speed denoted the speed of polymeric disc rotating against the steel pin.
- Sliding distance was the actual run-distance of the steel pin over the polymeric sample.
- The acquisition radius formed the radius of a circle subject to which the pin rotated over the sample.
- The Pin-on-Disc configuration had the property of surface contact whereas the Ball-on-Disc configuration had a point contact.

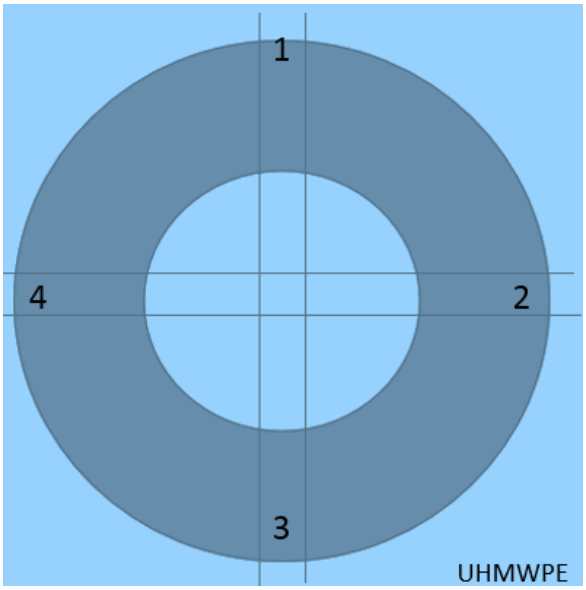

Figure 4.7. Spot-Marking on wear-scar of UHMWPE sample

The polymer-UHMWPE since cuboidal in shape had to be connected by a cylindrical disc beneath it as to facilitate rotation of the cuboid against the action of the steel pin. For this configuration, the illustration can be seen in the below, fig. 4.8. The disc assumed the shape of the

cavity and the tribological properties were thus measured upon revolution of the polymer in attachment to the disc.

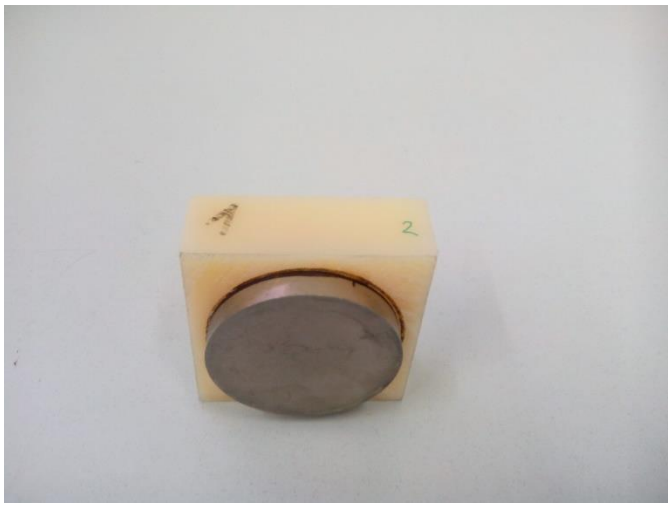

Figure 4.8. Cylindrical Cavity attachment

4.1.4 Observations and Analysis

Considering these properties the following tests in the table were conducted. The contact pressures were calculated using the Hertzian contact theory as previously described, see chapter 3, fig. 3.1 and fig. 3.6. Every test was done at a different acquisition radii to prevent overriding results.

Table 4.3. Tribological Optimization Testing Observations

Sample/Test	Vertical Load	Linear Speed	Distance	Acquisition Radius	Configuration Type	Contact Pressure	Wear Scar Depth
Sample2/Test-1	6N	0.7m/s	25km	18mm	Pin-on-Disc	0.85MPa	IS
Sample2/Test-2	25N	0.7m/s	25km	21mm	Pin-on-Disc	3.5MPa	IS
Sample2/Test-3	1N	0.7m/s	10km	14mm	Ball-on-Disc	13MPa	IS
Sample2/Test-4	10N	0.7m/s	10km	25mm	Ball-on-Disc	29MPa	S
Sample2/Test-5	10N	1m/s	10km	27.5mm	Ball-on-Disc	29MPa	S
Sample2/Test-6	10N	1m/s	25km	16mm	Ball-on-Disc	29MPa	S

IS: Insignificant Wear-Scar Depth, S: Significant Wear-Scar Depth.

- Under preliminary testing of tribological optimization (see, table 4.3), the initial reference sample (Sample2, randomly chosen) was subjected under conditions of a vertical load of 6 N with a Pin-on-Disc configuration. The acquisition radius was chosen as 18 mm and linear speed 0.7 m/s. The test was set to run for 25 km after which the wear plot was adjudged to note if there was significant amount of abrading. The wear-plot yielded an immeasurably low level of wear content that was *Insignificant*, also shown by the graph in fig. 4.9 (detailed explanation of wear-plot presented below) and thus it was necessary to further vary a parameter (load) for better indication of wear on the UHMWPE sample.
- Thus the load was proliferated from 6 N to 25 N all the other parameters being the same. The second case (Sample2/Test-2) yielded a similar plot as the first case with really low degree of wear which in other words indicated that the Pin-on-Disc configuration was performing poorly thus the successive tests had to be done with a Ball-on-Disc configuration. This meant a higher contact pressure (Sample2/Test3, 13 MPa) with higher probability of mushroomed wear with increase in load and sliding velocity. (Sample2/Test-4, Test-5 and Test-6).
- The Pin-on-Disc configuration yielded *Insignificant* wear scars whereas the Ball-on-Disc configuration with exception to Sample2/Test-3 yielded *Significant* wear scars, that is described in detail, below.
- The HOMMEL Profilometer facilitated the graphical representation of the wear-scar in specific detail for tribological optimization. (see, fig. 4.9, fig. 4.10, fig. 4.11)

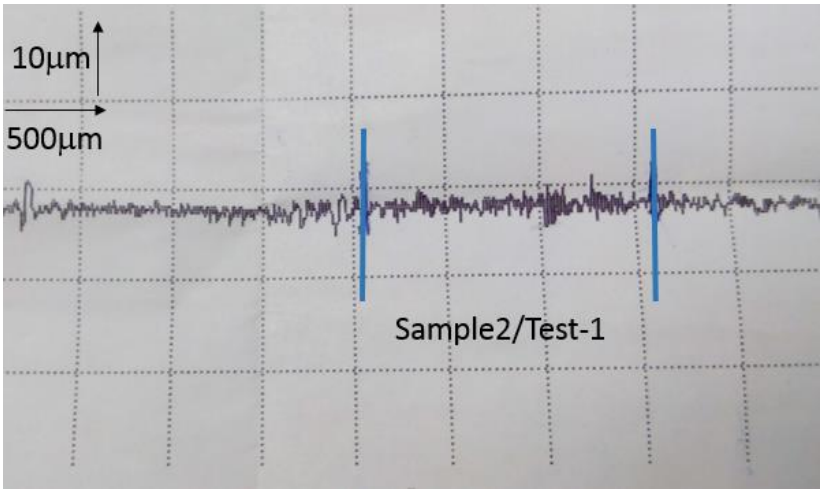

Figure 4.9.Insignificant wear as for Sample2/Test-1 indicated by the wear-plot.

- Therefore extending the principle to a vertical load to 10 N (Sample2/Test-4), with contact pressure more than double compared to the previous case, the following wear scars were obtained, see fig. 4.10. To further improve the measurable wear the sliding velocity was varied, all the parameters with exception to the acquisition radii being the same.
- Velocity of sliding was increased from 0.7 m/s to 1 m/s (Sample2/Test-5) have a higher wear-depth. The graphical plots of the tests 4 and 5 as described below.
- The Sample2/Test-5 had a higher depth (~7.5 µm) in comparison to Sample2/Test-4 that had a lower depth (~5 µm).

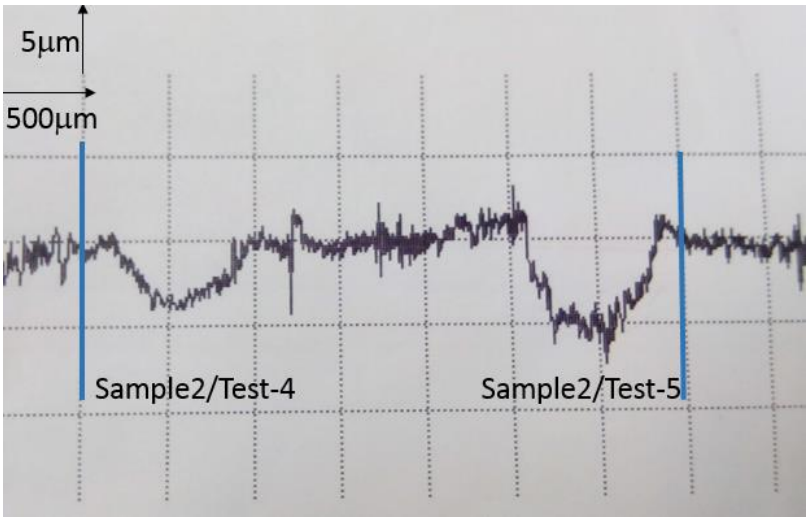

Figure 4.10.Significant wear as for Sample2/Test-4 and Test-5 indicated by the wear-plot.

- Now that the interim tribological-optimization was done (Sample2/Test-5), to better comprehend the wear process, the sliding-distance was increased from 10 km to 25 km.
- The Sample2 in tribological –optimization operation had a maximum run time of about 8 hours during which the equipment was left to function automatically.
- The final test had the highest wear depth (~9 µm), see fig. 4.11, and this was taken as the tribologically optimized state with measurable and definite wear scar characteristics.
- Using the results of the tribological optimization, it was extended to the other samples one, three and four (Sample1, Sample3 and Sample4) and Sample2 itself, for measurement of friction coefficient (COF) and normalized wear rate (NWR).

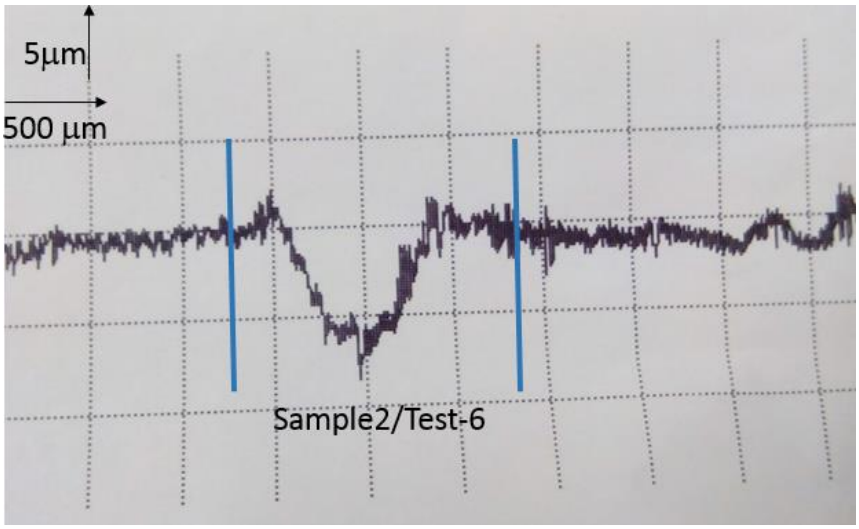

Figure 4.11.Significant wear as for Sample2/Test-6 indicated by the wear-plot.

- Thus Test-6 had the tribologically optimized condition with parameters relating to; Hertzian Contact Pressure: 29 MPa, Vertical Load: 10 N and Sliding Distance: 25 km and Velocity of Sliding: 1 m/s.

4.2 SECONDARY TESTING

4.2.1 Analysis of Friction Coefficient

- In the first section of the secondary testing, friction coefficients are analyzed in detail. The specimens have a run distance of 25000 m (25 km) [Sample2/Test-6] from the tribological-optimization procedure.
- Within this, our area of interest is the stable region of COF which is taken from 10000 m (10 km) to 20000 m (20 km). The test consisted of two runs at different acquisition radii and the values of COF are recorded at every distance-interval.
- An excerpt into the values of the run-distance and COF is provided below. As tabular conclusion, average friction coefficient and standard deviation is presented in the part found below, see table 4.4.

Table 4.4. COF vs Sliding Distance Observations

Distance (m) *(Sample1 @ 25mm)*	COF (No unit)	Distance (m) *(Sample2 @ 25mm)*	COF (No unit)	Distance (m) *(Sample3 @ 25mm)*	COF (No unit)	Distance (m) *(Sample4 @ 25mm)*	COF (No unit)
10000.42	0.12372	10007.79	0.12449	10002.34	0.10511	10002.25	0.18295
10010.32	0.12362	10017.68	0.12463	10012.4	0.10458	10012.3	0.18303
10020.37	0.1233	10027.74	0.12433	10022.45	0.10476	10022.2	0.18405
10030.42	0.12376	10037.79	0.12395	10032.5	0.10499	10032.26	0.18438
10040.32	0.12306	10047.69	0.12392	10042.4	0.10478	10042.31	0.1841
19043.32	0.14216	19042.43	0.12316	19035.74	0.10908	19034.77	0.18048
19053.38	0.14167	19052.32	0.12285	19045.64	0.10896	19044.66	0.18067
19063.27	0.14168	19062.38	0.1228	19055.69	0.10841	19054.72	0.18115
20003.35	0.13374	20003.32	0.12294	20006.1	0.11044	20004.81	0.17516
Distance (m) *(Sample1 @ 27.5mm)*	COF (No unit)	Distance (m) *(Sample2 @ 27.5mm)*	COF (No unit)	Distance (m) *(Sample3 @ 27.5mm)*	COF (No unit)	Distance (m) *(Sample4 @ 23mm)*	COF (No unit)
10016.99	0.10703	10005.57	0.12544	10005.99	0.10419	10009.44	0.21123
10027.02	0.10715	10015.59	0.12554	10016.02	0.10445	10019.41	0.21158
10037.04	0.10736	10025.62	0.12494	10025.87	0.10433	10029.39	0.21148
10047.06	0.10718	10035.64	0.1248	10035.89	0.104	10039.51	0.20875
10057.09	0.10694	10045.66	0.12472	10045.91	0.10478	10049.48	0.20852
19968.48	0.10943	19956	0.12879	19942.87	0.10549	19957	0.18589
19978.5	0.10884	19966.02	0.1283	19952.72	0.10527	19966.97	0.18683
20008.4	0.10821	20006.12	0.13016	20002.66	0.10548	20006.88	0.18791
Avg. COF	**0.118**	**Avg. COF**	**0.127**	**Avg. COF**	**0.107**	**Avg. COF**	**0.186**
Std. Dev.	**0.0106**	**Std. Dev.**	**0.0028**	**Std. Dev.**	**0.0023**	**Std. Dev.**	**0.0095**

There were a set of two tests which were applied per sample at different acquisition radii due to data scattering. Taking into account the first sample (Sample1) the acquisition radius was set at 25mm (primary run) and 27.5mm (secondary run). The objective now was to conduct the tests with the specification mentioned as in the final test of the second sample (Sample2/Test-6). The Ball-on-Disc configuration was employed and the coefficient of friction was noted for a plot alongside the run-distance and we had the following result, see fig.4.12.

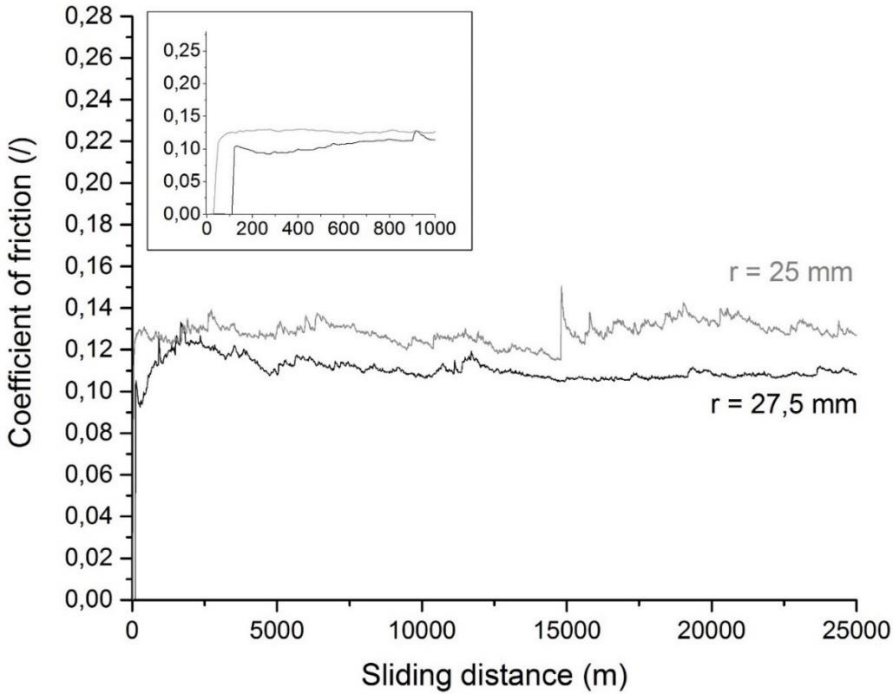

Figure 4.12. Sliding distance (m) vs COF, UHMWPE Sample 1

The initial part of its friction characteristics has been appended on the upper portion of the plot. This indicates the gradual increase of friction due to loading, with sliding distance, followed by a near-constant characteristic (10 km to 20 km). Our interest was to gauge the region of near-constant characteristics, therefore the inconsistent values of friction are not taken into consideration. For the acquisition radius of 25 mm comparatively higher COF was observed. At 27.5 mm on the polymer-UHMWPE, the COF increased to a little above 0.12, being the apex point. The values of coefficient of friction (COF) obtained here was 0.118 (i.e. UHMWPE/Steel), was similar to combinations of UHMWPE/Steel and UHMWPE/AISI420C Steel, from literature, whose ranges were from 0.113-0.213 and 0.103-0.123 respectively, see Table 3.1. The wear observed was predominantly abrasive in nature and standard deviation recorded was 0.0106, see table 4.4.

The fig. 4.13, shows the plot between COF and sliding distance for Sample2. The acquisition radius for the second sample here was chosen at radii at 25 mm (primary run) and 27.5mm (secondary run). The tests revealed the following results:

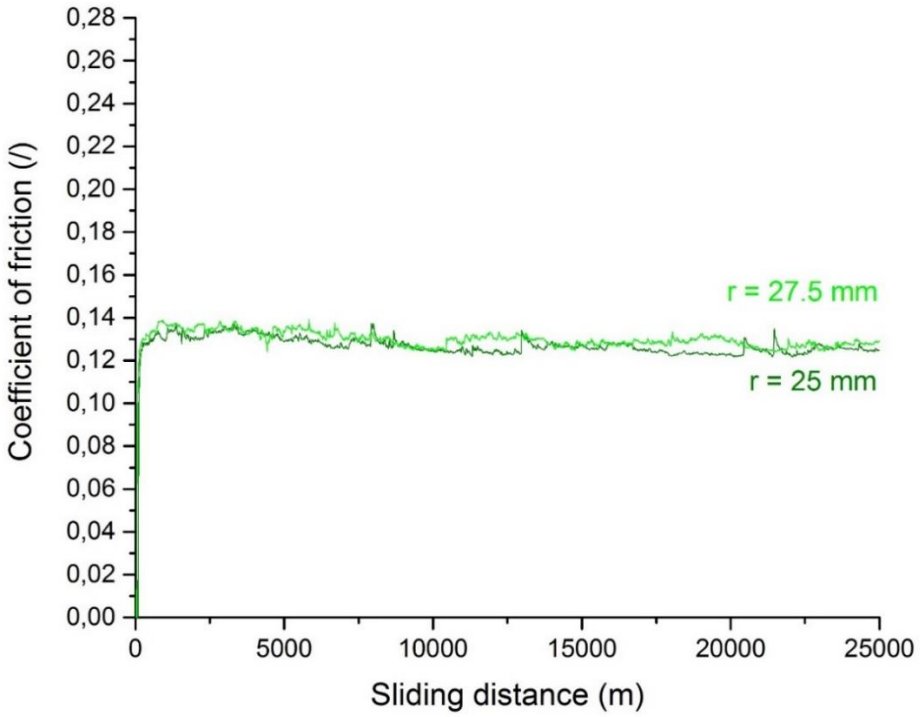

Figure 4.13. Sliding distance (m) vs COF, UHMWPE Sample 2

It could be noted that the for the primary-run at 25mm the coefficient of friction was in the range of 0.12 to a little above 0.13 and in the secondary run at 27.5mm the coefficient of friction was still slightly higher, similar in nature though. The primary and secondary runs have less standard deviation (0.0028) and the coefficient of friction (0.127) was recorded for final comparison.

The results of COF were comparable with values obtained from combinations of UHMWPE/AISI316L Steel and UHMWPE/Steel whose ranges are from 0.125-0.138 and 0.113-0.213 respectively, see Table 3.1. Noticeably AISI316L in combination with UHMWPE was observed to have near-similar characteristics as the former. The wear process that took place was abrasive in nature with scratch marks on the surface of the polymer-UHMWPE.

The fig. 4.14, shows the plot between COF and sliding distance for Sample3. Extending the testing principle to the third sample the acquisition radius was defined at 25 mm (primary run) and 27.5 mm (secondary run). The coefficient of friction for the primary run at r=25 mm, yielded quite a formidable result when compared to the other samples with a COF range from 0.09 to a little less than 0.11.

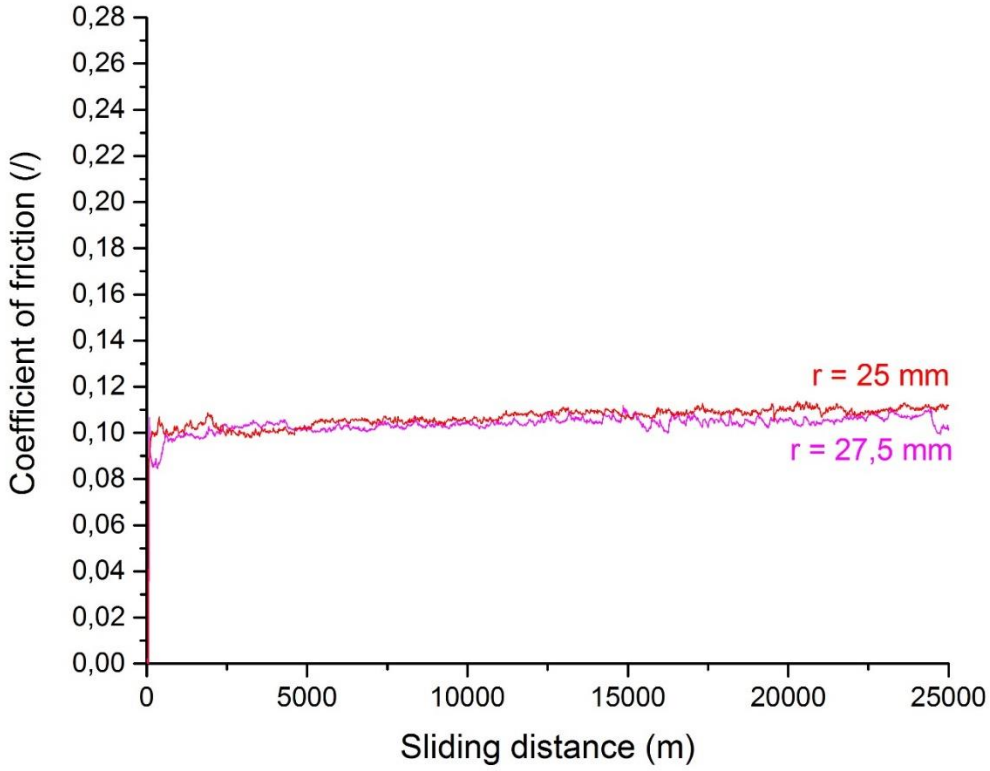

Figure 4.14. Sliding distance (m) vs COF, UHMWPE Sample 3

The second run was taken at a radius of 27.5 mm and it was found to have similar characteristics and the standard deviation was 0.0023 from the primary-run was not too offset which was quite an advantage compared to Sample1 and Sample2. The average friction coefficient was found to be 0.107 which was comprehended to be quite low. The results were quite appreciable.

The values of COF were found to be similar to the combinations of UHMWPE/$Zr0_2$ and UHMWPE/AISI420C Steel whose ranges were from 0.04-0.12 and 0.103-0.123 respectively. These are the lowest values of friction coefficient as from Table 3.1. Similar to the previous cases the wear obtained here was also abrasive in nature from the wear-surface definitions of the polymer.

Considering the final sample (Sample4), see fig. 4.15, the primary run was made at the first acquisition radius (r= 25 mm) and the second run at acquisition radius (r= 23 mm). The observations made were as follows:

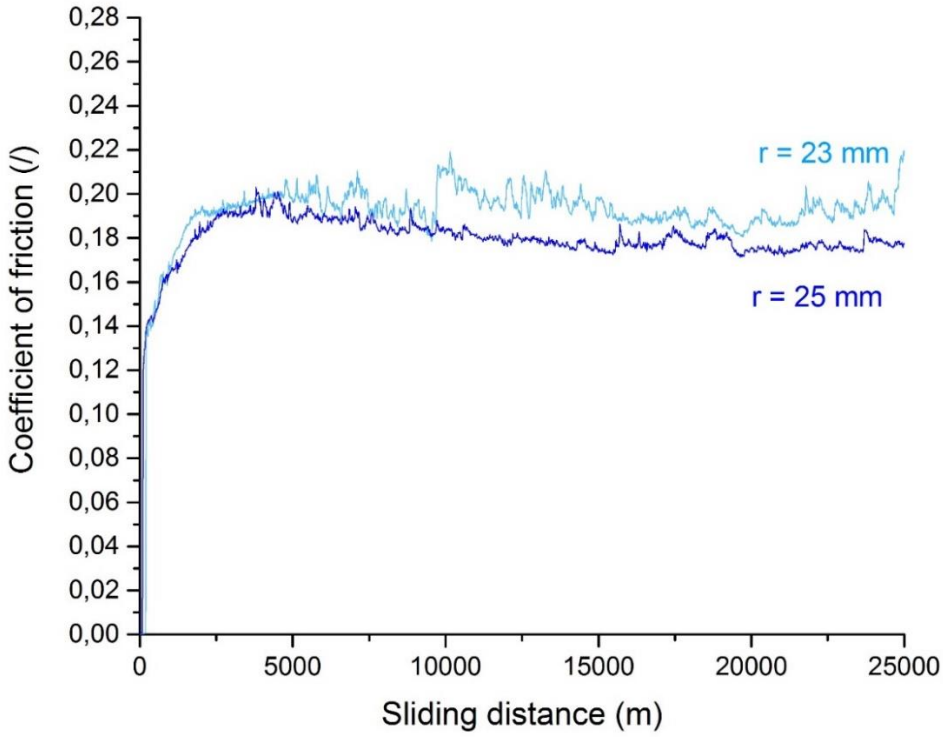

Figure 4.15. Sliding distance (m) vs COF, UHMWPE Sample 4

It was noted that the second-run (r= 23 mm) had a similar COF to the primary run (r= 25 mm) initially, but picked up and the overall comparative standard deviation of the two runs was large (0.0095). The average friction coefficients (0.186) in this case were definitely quite higher also comparing it to the tribo-runs of the other samples and it can be predicted that the corresponding wear rate would also be humongous. The values of COF are noticeably similar to the combinations of UHMWPE/CoCr and UHMWPE/ Steel whose ranges were from 0.185-0.210 and 0.113-0.213 respectively, see Table 3.1. Its characteristics were similar to sliding contacts with chrome alloys and steels with high degree of COF and thus predictably high degree of wear. The predominant wear in this case was abrasive, in addition to adhesive wear because of material transfer from the polymer to the steel counterface.

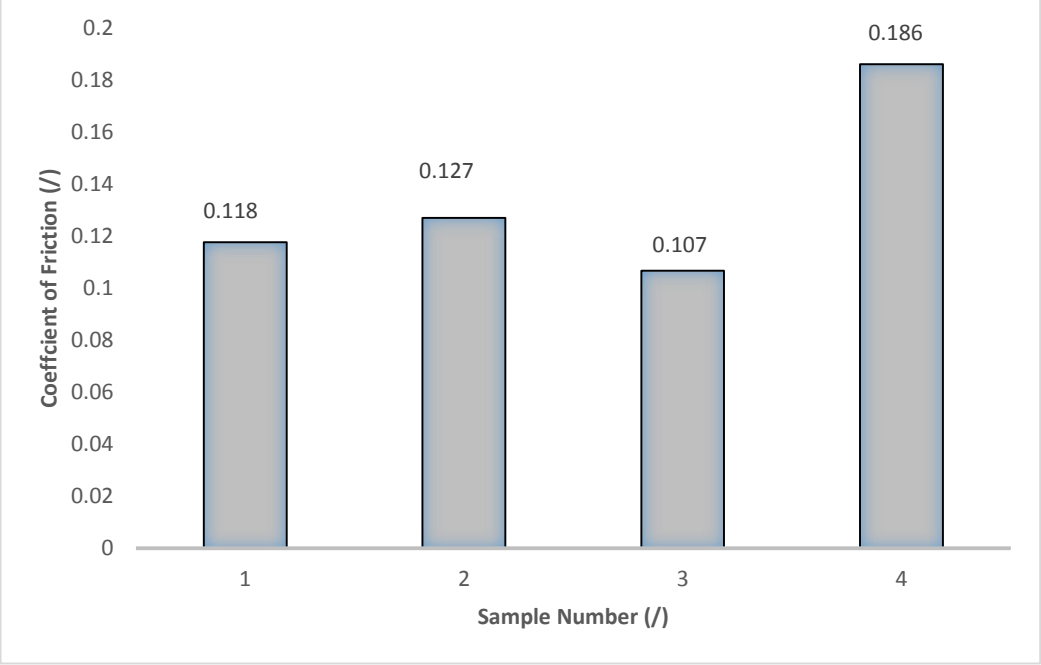

Figure 4.16. COF vs Sample

- The plots defining the average coefficient of friction, see fig.4.16, shows that COF (0.107) of the third sample (Sample3) was the least among the four. The third sample also had the least standard deviation (0.0023) considering the primary and secondary runs at different acquisition radii. Vacuum cooling that was used for processing the third sample (Sample3) had promoted a better surface finish and an intermolecular geometry that was quite ordered.
- The friction coefficient (0.118) of the first sample (Sample1) featured second best though it had a higher standard deviation (0.0106).
- Sample2 was subjected to prolonged cooling procedure to room temperature. The friction coefficient (0.127) was found to be higher than the former samples (Sample1 and Sample3) but had the second best standard deviation at 0.0028. This could most probably be due to change in polymerization process that proliferated the rate of COF.
- The case with prolonged cooling in vacuum (Sample4) had the worst COF (0.186) characteristics which was nearly 1.75 times the best-fit sample' COF (i.e. Sample3). This could be theorized because of poor surface definitions set in by lengthened cooling which had promoted micro-level molecular branching. The second largest standard deviation at 0.0095 was also observed.

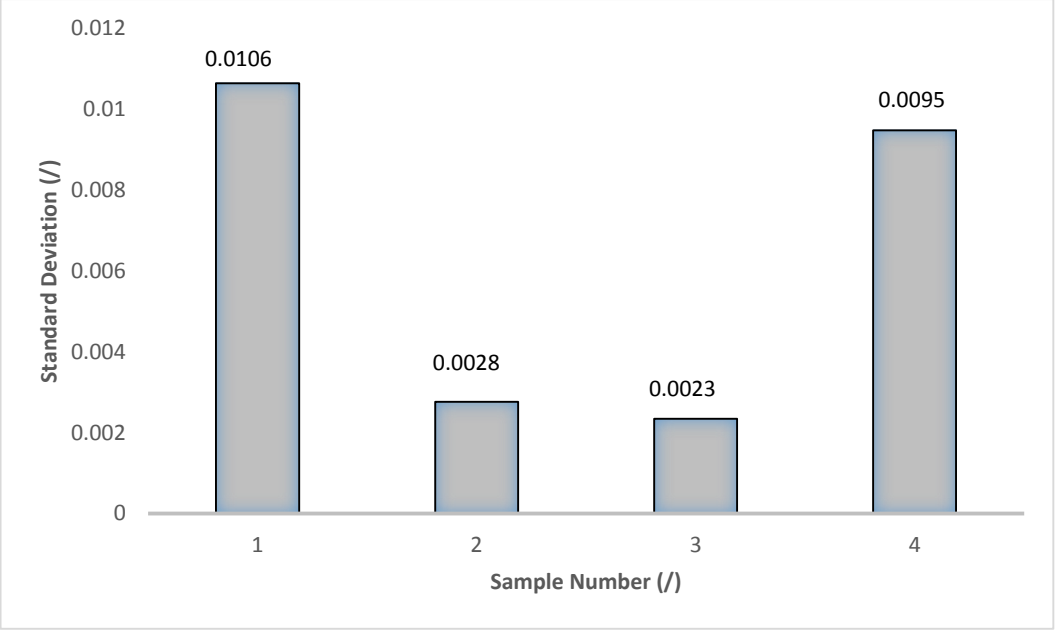

Figure 4.17. Std. dev. vs Sample (COF)

- In general prolonged cooling caused substandard surface finish which in turn spawned a higher friction coefficient. Differences in standard deviation (see, fig. 4.17) between the primary and secondary runs depicted that the fact that the polymer was uniformly processed. Sample3 had a surpassing surface-demarcation which denoted best superficial finish. In terms of friction coefficient; Sample3 had better characteristics than Sample1, Sample2 and Sample4 in respective precedence.

4.2.2 Analysis of Wear

- Wear was another important factor in the determination of the best-fit sample and for this the achieved normalized wear rates (NWR) for the four differently processed samples are statistically presented below, see Table 4.5 to Table 4.8.
- The normalized wear rate was calculated by taking into account the volume loss and the normalized load was 10N and run-distance was 25km (Sample2/Test-6) from the tribological-optimization condition. The wear-scar positions (see, fig. 4.7) had the corresponding volume losses as represented below.

Table 4.5. Acquisition Radius-Wear Scar Position-Volume Loss- NWR-Sample1

Acquisition Radius (mm)	Position of Wear-Scar in Spot-Marking	Volume Loss (mm^3)	Normalized Wear Rate NWR, (mm^3/Nm)
25.00	1	0.265650437	1.0626E-06
	2	0.234851433	9.39406E-07
	3	0.18053273	7.22131E-07
	4	0.273046864	1.09219E-06
27.50	1	0.260099843	1.0404E-06
	2	0.247795314	9.91181E-07
	3	0.228775517	9.15102E-07
	4	0.239769772	9.59079E-07
		Average NWR	**0.97E-06**
		Std. Dev.	**1.16E-07**

Table 4.6. Acquisition Radius-Wear Scar Position-Volume Loss- NWR-Sample2

Acquisition Radius (mm)	Position of Wear-Scar in Spot-Marking	Volume Loss (mm^3)	Normalized Wear Rate NWR, (mm^3/Nm)
25.00	1	0.286876052	1.1475E-06
	2	0.350610516	1.40244E-06
	3	0.311902794	1.24761E-06
	4	0.315794196	1.26318E-06
27.50	1	0.314929676	1.25972E-06
	2	0.397892683	1.59157E-06
	3	0.472641906	1.89057E-06
	4	0.411747886	1.64699E-06
		Average NWR	**1.43E-06**
		Std. Dev.	**2.55E-07**

Table 4.7. Acquisition Radius-Wear Scar Position-Volume Loss- NWR-Sample3

Acquisition Radius (mm)	Position of Wear-Scar in Spot-Marking	Volume Loss (mm^3)	Normalized Wear Rate NWR, (mm^3/Nm)
25.00	1	0.235219441	9.40878E-07
	2	0.203004454	8.12018E-07
	3	0.261643012	1.04657E-06
	4	0.212298226	8.49193E-07
27.50	1	0.263341595	1.05337E-06
	2	0.235379911	9.4152E-07
	3	0.230351232	9.21405E-07
	4	0.186251424	7.45006E-07
		Average NWR	**0.91E-06**
		Std. Dev.	**1.08E-07**

Table 4.8. Acquisition Radius-Wear Scar Position-Volume Loss- NWR-Sample4

Acquisition Radius (mm)	Position of Wear-Scar in Spot-Marking	Volume Loss (mm^3)	Normalized Wear Rate NWR, (mm^3/Nm)
25.00	1	0.465906135	1.86362E-06
	2	0.529394737	2.11758E-06
	3	0.459449039	1.8378E-06
	4	0.380966466	1.52387E-06
23.00	1	0.551300325	2.2052E-06
	2	0.627702152	2.51081E-06
	3	0.594150762	2.3766E-06
	4	0.585799097	2.3432E-06
		Average NWR	**2.10E-06**
		Std. Dev.	**3.32E-07**

In order to compare the four samples there were a set of three plots that define the imperativeness of this test:

- Normalized Wear Rate (NWR) vs Sample
- Standard Deviation vs Sample
- Volume Loss vs Sample wear-scar position.

By virtue of the first plot the wear rate of the four samples was judged and the sample that had the lowest wear was determined for its feasibility in applications. The second plot and third plot show the uniformity of material composition after the post-processing conditions.

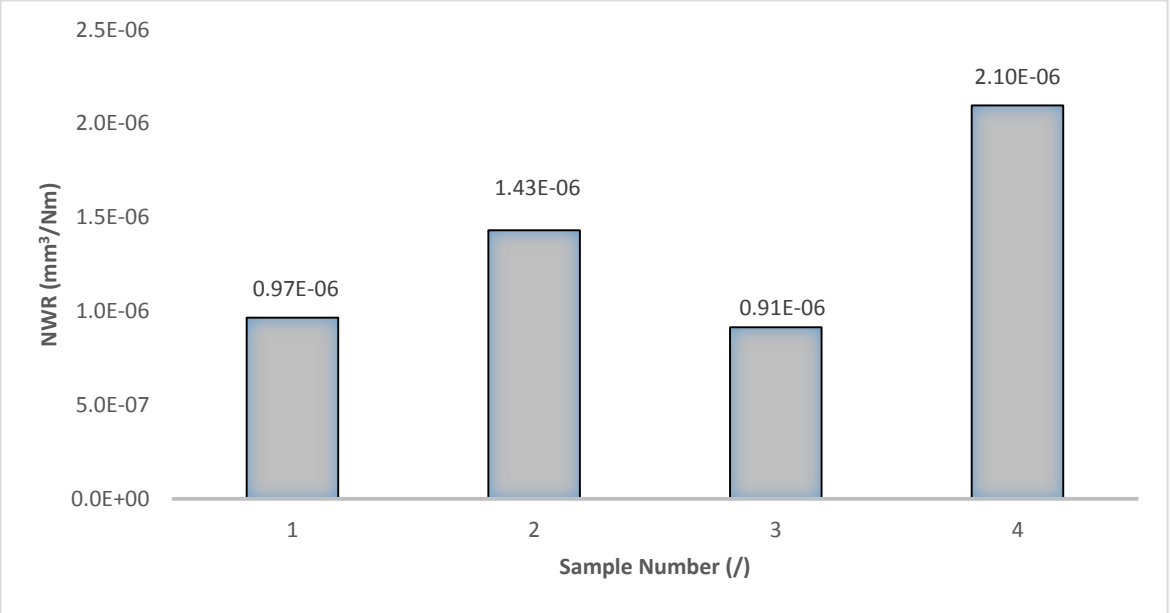

Figure 4.18. Wear Rate (mm^3/Nm) vs UHMWPE Sample

- The first sample (Sample1) had a lower wear rate (0.97E-06), see fig.4.18. It had better wear-resistant properties than the second sample (Sample2, 1.43E-06). The third sample (Sample3) had relatively the lowest wear in comparison to the other three samples (0.91E-06). Thus vacuum which was devoid of temperature, humidity and pressure changes yielded the lowest wear rate. It could be observed that prolonged cooling did not yield significant positive wear-resistant results, although assumed it would accommodate better space-time-geometry relationship in the micro-molecular restructuring. The precedence of the standard deviation values were: Sample3 (1.08E-07), Sample1 (1.16E-07), Sample2 (2.55E-07) and Sample4 (3.32E-07), see fig. 4.19, which was the same with the case of NWR, previously mentioned.

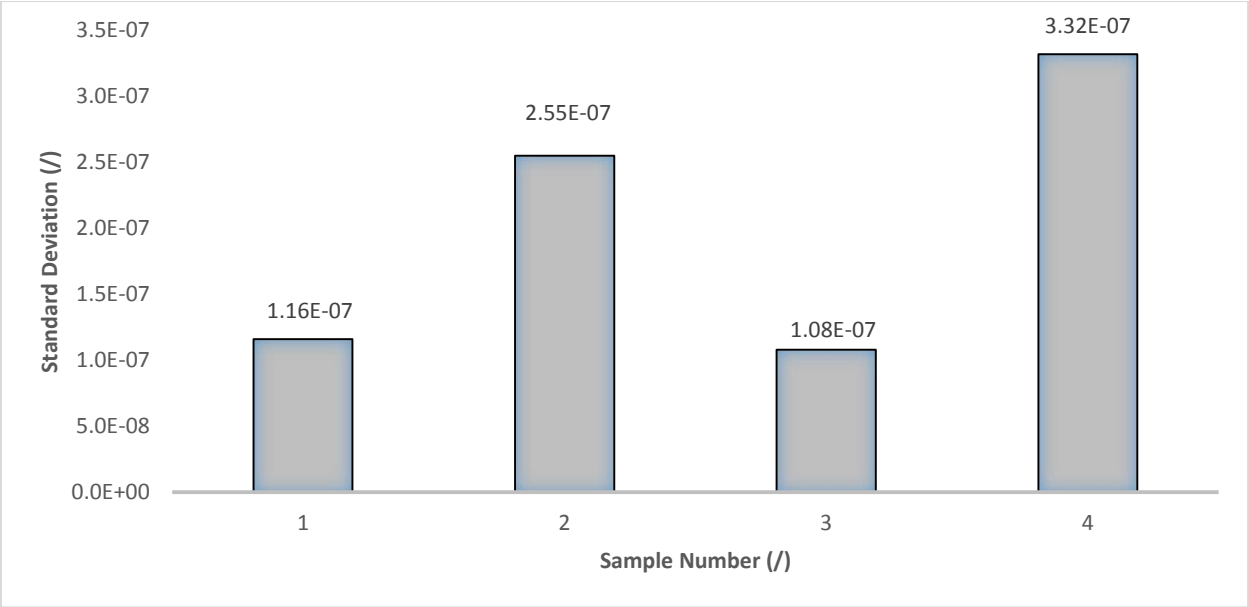

Figure 4.19. Std. dev. vs Sample (NWR)

- Considering volume loss at different positions of the wear scar of Sample 1 (see, fig. 4.20) it was found to vary quite non-uniformly. The wear scar at position-3 (Volume-loss [Sample1_25mm]: 0.18 mm^3) and Volume-loss [Sample1_27.5mm]: 0.23 mm^3) for Sample1 was found to have the highest wear resistance in comparison to the other positions. This indicates the material distribution was uniform in this region.

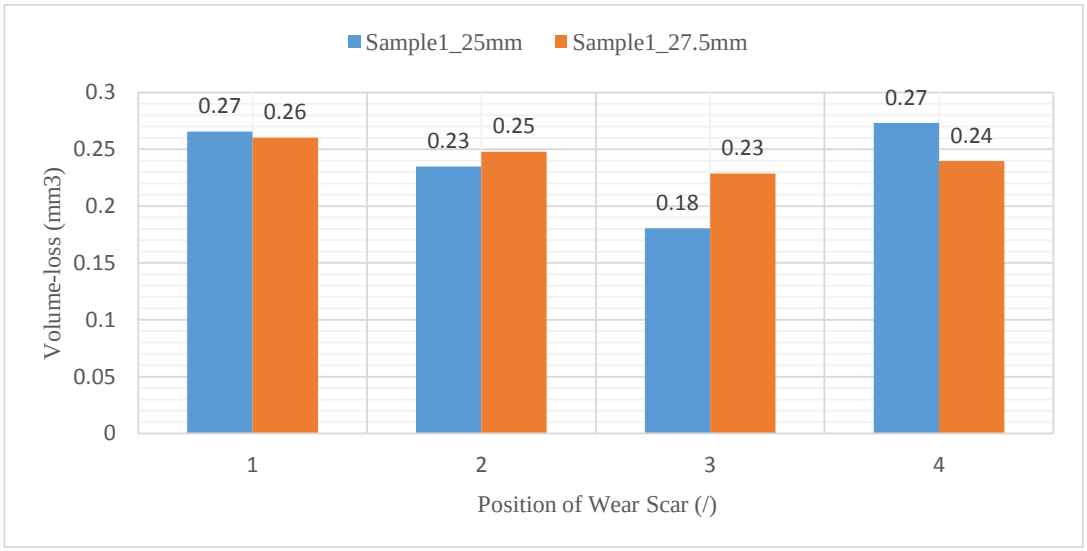

Figure 4.20. Volume Loss Plot- Sample1

- In Sample2 (see, fig. 4.21) the highest wear resistance was at position-1 (Volume-loss [Sample1_25mm]: 0.29 mm^3) and in the case of the secondary run at 27.5 mm it was also at position-1 (Volume-loss [Sample2_27.5mm]: 0.31 mm^3). This generally indicates the varying consistency of post-processing finish of the polymer.

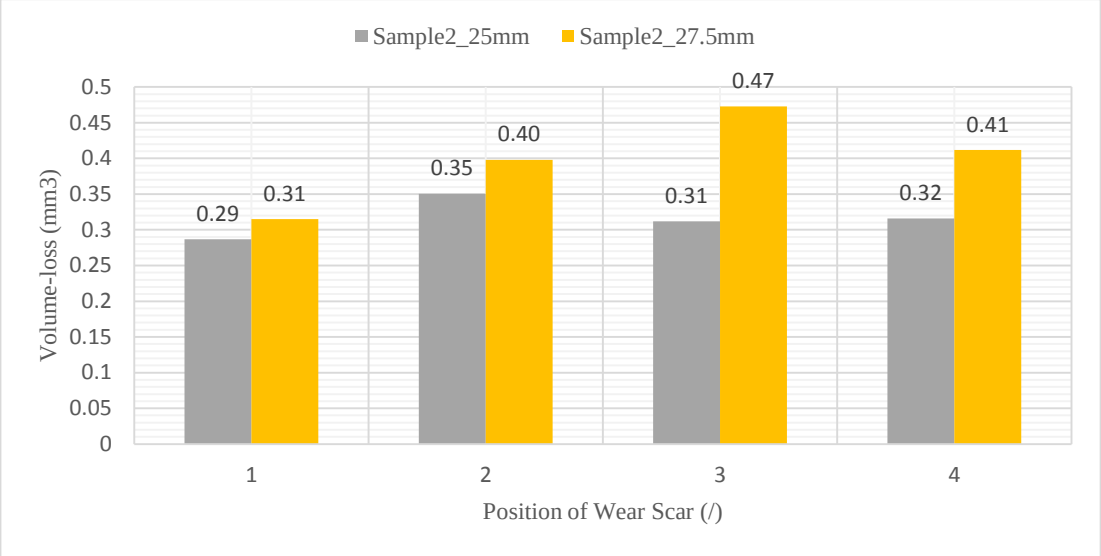

Figure 4.21. Volume Loss Plot- Sample2

- Sample3 (see, fig. 4.22) was found to be best sample in terms of both friction coefficient and wear resistance and this was quite evident from the results of the volume loss at different positions which had lesser standard deviation indicating better material finish . The sample had highest wear resistances at position-2 (Volume-loss [Sample3_25mm]: 0.20 mm^3) and at position-4 (Volume-loss [Sample3_27.5mm]: 0.19 mm^3).
- Sample3 had the least coefficient of friction, lowest degree of normalized wear rate, a short standard deviation between primary and secondary run and lowest volume loss characteristics.
- The sample had a uniform material distribution which is quite an important result in final-processing.
- This sample due to its low friction coefficient and superior wear resistance characteristics can be proposed to be used in high performance bearings with COF from 0.04 – 0.12, which also require the polymer to withstand a high degree of wear.

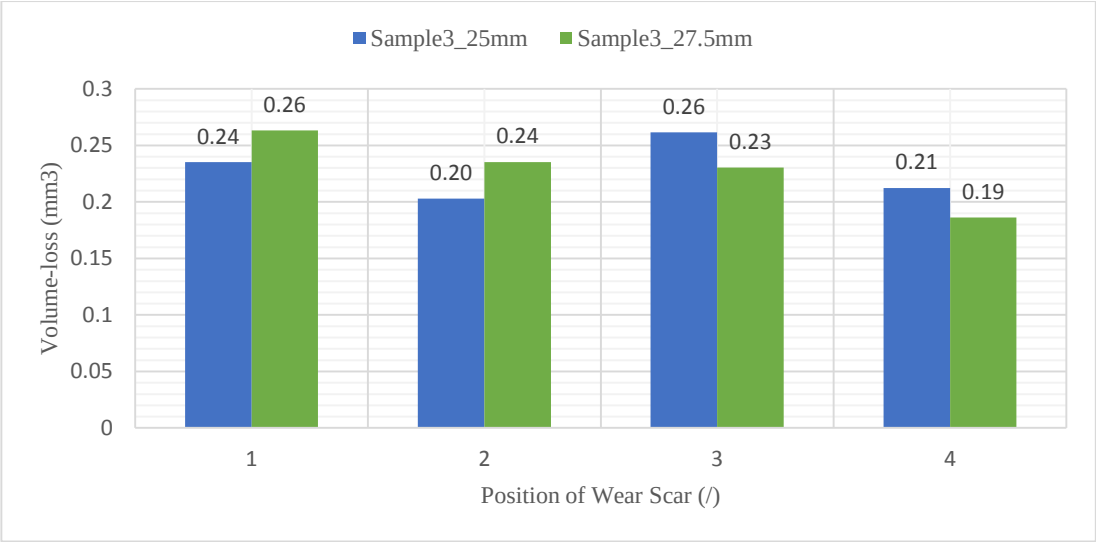

Figure 4.22. Volume Loss Plot- Sample3

- The highest wear resistance in Sample4 (see, fig. 4.23) was observed at position-4 (Volume-loss [Sample4_25mm]: 0.38 mm^3) and at position-1 (Volume-loss [Sample4_23mm]: 0.55 mm^3).
- This sample was found to have the worst tribological properties of the four. Prolonged cooling had deleterious effects and results upon sliding between the polymeric and metallic contacts.

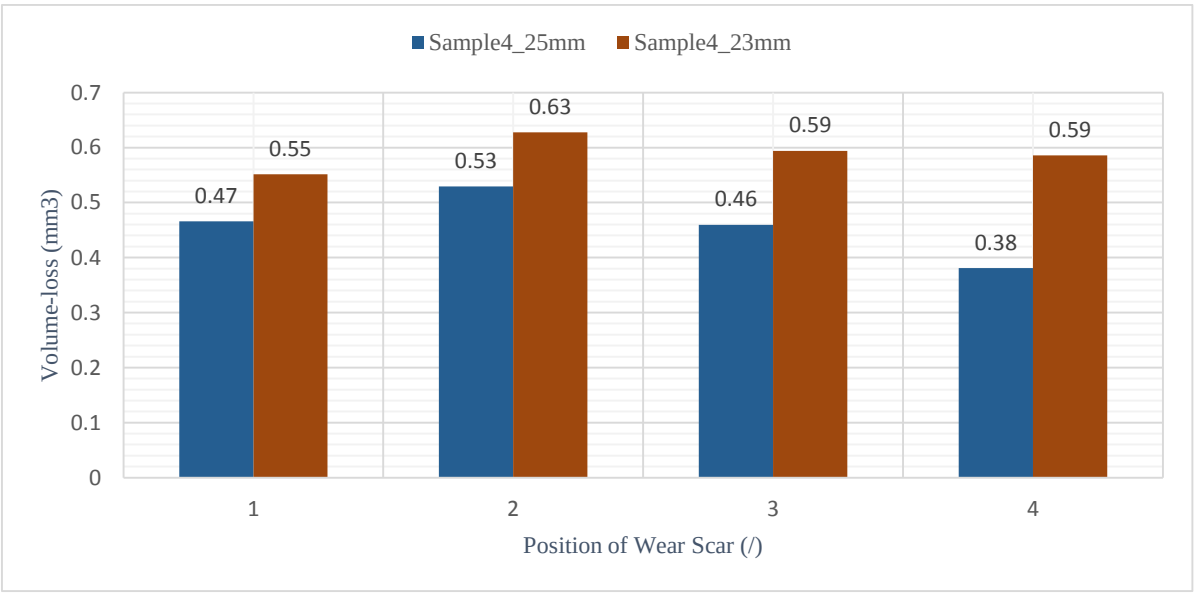

Figure 4.23. Volume Loss Plot- Sample4

As previously mentioned, the intent of this experimental work was to gauge the best sample out of the four, subject to different final processing conditions which were standard cooling to room temperature (Sample1), prolonged cooling to room temperature (Sample2), standard cooling in vacuum (Sample3) and prolonged cooling in vacuum (Sample4). Now juxtaposing COF and NWR in the form of a histogram (fig. 4.24) to also study the friction and wear-performance characteristics the overall observation would be the following:

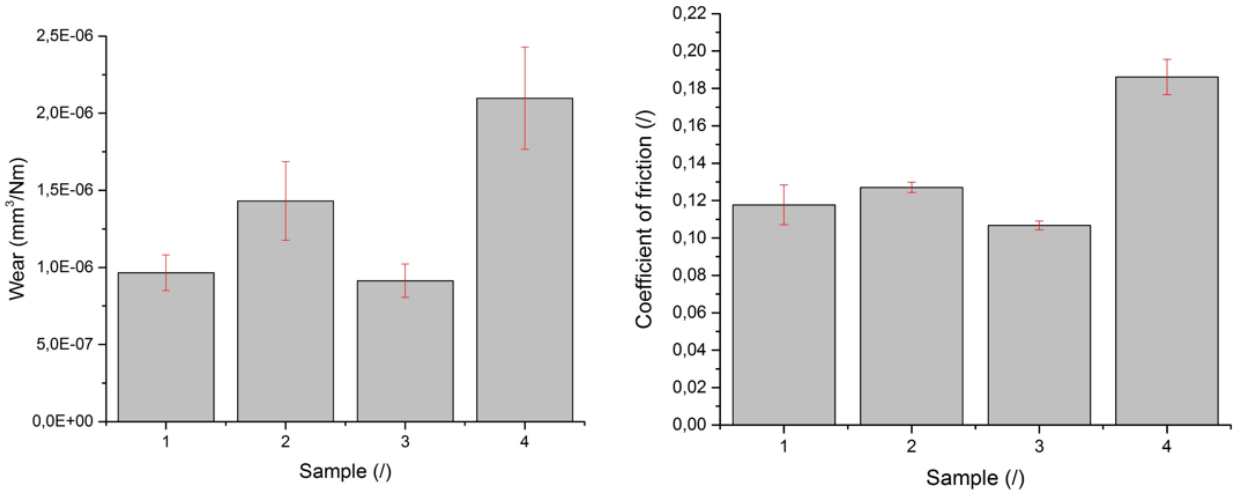

Figure 4.24. Histogram-comparison of Wear (Left) and COF (Right) vs UHMWPE samples

It was observed that COF and NWR was the least for the third sample (Sample3). It was also noted that the error bars denoting the standard deviation are the least for the third sample which are quite a calibre, denoting relatively finer material finish and uniform processing. Cooling down in vacuum was observed to have better tribological properties than that of the standard cooling down to room temperature (i.e. Sample3 better than Sample1). Even though prolonged cooling procedure was expected to produce better results considering enhanced symmetric-rearrangement of molecules and better energy-balance promoting equilibrium with time, the principle in theory worsened. The case of Sample2 (prolonged cooling to room temperature) was unmeritorious, worse still with the Sample4 (prolonged vacuum cooling) compared to other samples both in terms of friction coefficient (COF) and normalized wear rate (NWR). (i.e. Sample2 better than Sample4).

CONCLUSION AND RECOMMENDATION

1. The Pin-on-Disc configuration is a simple configuration that is used largely for Tribo-testing but the demerit is that it simulates only to an extent the friction and wear characteristics, and fails in some cases (Sample2/Test-1 and Test-2), in these exigencies the next level of intricacy is employed i.e. Ball-on-Disc configuration or other configurations.
2. The best-fit sample in terms of average friction coefficient and normalized wear rate is in the order of precedence:
   Sample3 (Standard Cooling in Vacuum | COF: 0.107 | NWR: 0.91 x 10^{-6} mm^3/Nm) > Sample1 (Standard Cooling to Room Temperature | COF: 0.118 | NWR: 0.97 x 10^{-6} mm^3/Nm) > Sample2 (Prolonged Cooling to Room Temperature | COF: 0.127 | NWR: 1.43 x 10^{-6} mm^3/Nm) > Sample1 (Prolonged Cooling in Vacuum | COF: 0.186 | NWR: 2.10 x 10^{-6} mm^3/Nm).
3. Since the third sample (Sample3) that was vacuum cooled had the least values of average friction coefficient (0.107) and normalized wear rate (0.91 x 10^{-6} mm^3/Nm), this therefore can be proposed to be used in high performance bearings with friction coefficients in the range of 0.04 – 0.12.
4. Vacuum cooling has the advantage of being devoid of the effects of temperature, pressure & humidity variations. It is quite suitable for customized applications with a need for high surface finish, but since vacuum cooling as such is expensive in nature, it may not always be feasible to employ it.
5. The samples that had prolonged cooling rates (Sample2 and Sample4) had the highest degree of friction coefficients and wear rates. Prolonged cooling, though typically expected of it to produce better crystallinity thus withstand wear, had an altogether different effect in this study. It caused detrimental effects in material properties as observed from the tribological tests. The reason might be attributed to change in polymerization-mechanism during lengthened cooling.

BIBLIOGRAPHY

[1] HARRIS, Frank. W., *Introduction to Polymer Chemistry*, Wright State University, Dayton. OH 45435, Nov 1981, p. 837-843, Vol 58 No 11.

[2] STACHOWIAK, Engineering Tribology, Elsevier Butterworth Heinemann Publisher, 2005. 775 p., ISBN 978-0750678360.

[3] MALUJDA, I., WILCZNSKI, D., Mechanical properties investigation of natural polymers, *Procedia Engineering*. 2016, 136, p. 263-268.

[4] GROSSIORD, N., Functional surfaces on performances polymers, *Materials Today: Proceedings 3*. 2016, 303-307.

[5] MYSHKIN, N.K., PETROKOVETS, M.I., KOVALEV, A.V., Tribology of polymers: Adhesion, friction, wear, and mass-transfer, *Tribology International*. 2005, 38, p. 910-921.

[6] FEYZULLAHOGLU, E., SAFFAK, Z., The tribological behaviour of different engineering plastics under dry friction conditions, *Materials and Design*. 2008, 29, p. 205-211.

[8] ZSIDAI, L., BAETS, P.D., SAMYN, P., KALACSKA, G., PETERGHEM, A.P.V., PARYS, F.V., The tribological behaviour of engineering plastics during sliding friction investigated with small-scale specimens, *Wear*. 2002, 253, p. 673-688.

[9] ZANG, J., ZHU, Z., SUN, H., LIANG, W., LI, A., Synthesis of functional conjugated microporous polymers containing pyridine units with high BET surface area for reversible CO2 storage, *Reactive and Functional Polymers*. 2016, 99, p. 95-99.

[10] ZHANG, S.W, State of the art of polymer tribology, *Tribology International*, 1998, 31, p. 49-60.

[11] OMRANI, E., MENEZES, P.L., ROHATGI, P.K., State of the art on tribological behavior of polymer matrix composites reinforced with natural fibers in the green materials world, *Engineering Science and Technology, an International Journal*. 2016, 19, p. 717-736.

[12] THEILER, G., HUBNER, W., GRADT, T., KLEIN, P., FRIEDRICH, K., Friction and wear of PTFE composites at cryogenic temperatures, *Tribology International*. 2002, 35, p. 449-458.

[13] WANG, Q., ZHENG, F., WANG, T., Tribological properties of polymers PI, PTFE and PEEK at cryogenic temperatures in vacuum, *Cryogenics*. 20016, 75, p. 19-25.

[14] BONA, J.D., LAINO, S., PETTARIN, V., BROITMAN, E., DOMMARCO, R., FRONTINI, P., Differences in the sliding wear track patterns between UHMWPE/steel and UHMWPE/CNx pairs, *Procedia Materials Science*. 2012, 1, p. 329-336.

[15] SAMAD, M., SINHA, S.K., Mechanical, thermal and tribological characterization of a UHMWPE film reinforced with carbon nanotubes coated on steel, *Tribology International*. 2011, 44, p. 1932-1941.

[16] SAMAD, M.A., SATYANARAYANA, N., SINHA, S.K., Tribology of UHMWPE film on air-plasma treated tool steel and effect of PFPE overcoat, *Surface and Coatings Technology*. 2010, 204, p. 1330-1338.

[17] JIA, B.B., LI, T.S., LIU, X.J., CONG, P.H., Tribological behaviors of several polymer–polymer sliding combinations under dry friction and oil-lubricated conditions, *Wear*. 2007, 262, p. 1353-1359.

[18] SENATOV, F.S., BARANOV, A.A., MURATOV, D.S., GORSHENKOV, M.V., KALOSHKIN, S.D., TCHERDYNTSEV, V.V., Microstructure and properties of composite materials based on UHMWPE after mechanical activation, *Journal of Alloy and Compounds*. 2014, 615, p. S573-S577.

[19] WU, J., PENG, Z., Investigation of the geometries and surface topographies of UHMWPE wear particles, *Tribology International*. 2013, 66, p. 208-218.

[20] SAMAD, M., SINHA, S.K., Mechanical, thermal and tribological characterization of a UHMWPE film reinforced with carbon nanotubes coated on steel, *Tribology International*. 2011, 44, p. 1932-1941.

[21] BAHADUR, S., The development of transfer layers and their role in polymer tribology, *Wear*. 2000, 245, p. 92-99.

[22] MYSHKIN, N. K., PESETSKII, S.S., GRIGORIEV, A.Y., *Polymer Tribology: Current State and Applications*, Vol.37 No. 3 (2015), p. 284-290.

[23] P.SAMYN, Wear transitions and stability of polyoxymethylene homopolymer in highly loaded applications compared to small-scale testing, *Tribology International*. 2007, 40, p. 819-833.

[24] WRIGHT, N.A., KUKUREKA, S.N., Wear testing and measurement techniques for polymer composite gears, *Wear Processes*. 2001, 251, p. 1567-1578.

[25] FERRAMOLA, E., GIACOMOZZI, G., Choice and Optimization of a tecno-polymer for planet wheels: Importance of the integration between material and design for plastic gears, *International VDI Conference on High Performance Plastic Gears*, München, 05.10.2015.

[26] CZYBORRA, L., FLOCK, J., CELANESE, Q.Z., Future solutions of polyacetal for gears at dry running conditions, *International VDI Conference on High Performance Plastic Gears*, München, 05.10.2015.

[27] CAMERA, D.L., VANDORMAEL, B., CATHELIN, J., Thermoplastic materials for gears: Status, future trends and solutions Material Science, Technology and Innovation, *International VDI Conference on High Performance Plastic Gears*, München, 05.10.2015.

[28] DRUMMER, D., GIERL, B., Possibilities and potential of plastics in gear applications, *International VDI Conference on High Performance Plastic Gears*, München, 05.10.2015.

[29] ABDELBARY, A., *Wear of polymers and composites*, Woodhead Publishing, 2014. 223 p., ISBN 978-1-78242-178-8.

[30] QU, J., ZHANG, Y., TIAN, X., LI, J., Wear behavior of filled polymers for ultrasonic motor in vacuum environments, *Wear*. 2015, 322-323, p. 108-116.

[31] UNAL, H., SEN, U., MIMAROGLU, A., Abrasive wear behaviour of polymeric materials, *Wear*. 2005, 26, p. 705-710.

[32] LANCASTER, J.K., Material-specific wear mechanisms: relevance to wear modelling, *Wear*. 1990, 141, p. 159-183.

[33] CZICHOS, H., Influence of adhesive and abrasive mechanisms on the tribological behaviour of thermoplastic polymers, *Wear*. 1983, 88, p. 27-43.

[34] GOLCHIN, A., WIKNER, A., EMAMI, N. An investigation into tribological behaviour of multi-walled carbon nanotube/graphene oxide reinforced UHMWPE in water lubricated contacts, *Tribology International*. 2016, 95, p. 156–161.

[35] *CSM Instruments* [interactive], [accessed on March 24th, 2016], *http://www.csm-instruments.com/fr/tests-Standards*.

[36] MENEZES, P.L., KAILAS, S.V. Role of surface texture and roughness parameters on friction and transfer film formation when UHMWPE sliding against steel, *Biosurface and Biotribology*. 2016, http://dx.doi.org/10.1016/j.bsbt.2016.02.001.

[37] RUGGIERO, A., D'AMOTO, R., GOMEZ, E., MEROLA, M. Experimental analysis of tribological behavior of UHMWPE against AISI420C and against TiAl6V4 alloy under dry and lubricated conditions, *Tribology International*. 2016, 92, p. 154-161.

[38] GUEZMIL, M., BENSALAH, W., MEZLINI, S. Effect of bio-lubrication on the tribological behavior of UHMWPE against M30NW stainless steel, *Tribology International*. 2016, 94, p. 550-559.

[39] RUGGIERO, A., D'AMOTO, R., GOMEZ, E., MEROLA, M. Experimental comparison on tribological pairs UHMWPE/TIAL6V4 alloy, UHMWPE/AISI316L austenitic stainless and UHMWPE/AL2O3 ceramic, under dry and lubricated conditions, *Tribology International*. 2016, 96, p. 349–360.

[40] HUANG, J., QU, S., WANG, J., YANG, D., DUAN, K., WENG, J. Reciprocating sliding wear behavior of alendronate sodium-loaded UHMWPE under different tribological conditions, *Materials Science and Engineering C*. 2013, 33, p. 3001–3009.

[41] CHANG, B.P., AKIL, H.M., NASIR, R.B., KHAN, A. Optimization on wear performance of UHMWPE composites using response surface methodology, *Tribology International*. 2015, 88, p. 252–262.

[42] *Laboratory for Tribology and Interface Nanotechnology* [interactive], [accessed on March 24th, 2016], *http://www.tint.fs.uni-lj.si/en*.